J. Membrane Biol. 38, 151 – 191 (1978)

Analysis of the Multi-pore System of Alamethicin in a Lipid Membrane

II. Autocorrelation Analysis and Power Spectral Density

Hans-Albert Kolb and Günther Boheim
Fachbereich Biologie, Universität Konstanz, D-7750 Konstanz, Germany

Received 12 November 1976

Summary. The properties of the alamethicin pore in multi-pore systems have been studied by autocorrelation analysis and by power spectral density. In agreement with the relaxation studies of part I, we found two processes of different time behavior and voltage dependency. The slow (sec) and fast (msec) correlation times could be related to fluctuations in the number of pores and to transitions between different levels of conductance within a pore, respectively. The interpretation of the correlation amplitudes in terms of a simplified three-state model used for the calculation of the corresponding unit step conductances confirms the assignment. The correlation amplitude of the slow process could be related to the mean single-pore conductance. The mean conductance difference of neighboring conducting pore states could be estimated using the product of the correlation amplitudes of the slow and fast process. In the range of weakly voltage-dependent conductance a strongly conductance-dependent increase of the correlation times as well as of the correlation amplitudes was observed. A conductance dependent on the size of the preaggregate from which the pore is formed was proposed for an interpretation of these findings. The mean single-pore conductance and the mean conductance difference of neighboring conducting pore states vary approximately linearly (on the log/log scale) on ion concentration in the range 0.1 to 1 M KCl. The salt concentration dependence of the macroscopic conductance was found to increase with decreasing temperature. An influence of the ionic strength on both correlation times could be observed.

It has been shown that the polypeptide antibiotic alamethicin induces voltage-dependent changes of the cation and anion permeability of lipid bilayers (Mueller & Rudin, 1968). From the statistical analysis of single-pore experiments it is already well established that the alamethicin-induced conductance arises from the presence of pores which are composed of several polypeptide molecules. The pores exhibit a pattern of discrete conductance states ordered in a consecutive sequence (Gordon & Haydon, 1972; Eisenberg, Hall & Mead, 1973; Boheim, 1974; Gordon & Haydon, 1976; Mueller, 1976).

022-2631/78/0038-0151 $8.20

Studies of single-pore fluctuations give evidence that the strong voltage-dependent conductance of lipid bilayers containing alamethicin is mainly related to the probability of pore formation, while the transition probabilities between different conducting states are comparatively little affected by the voltage (Eisenberg *et al.*, 1973; Boheim, 1974; Gordon & Haydon, 1975). From voltage-jump current relaxation experiments with lipid membranes containing a large number of alamethicin pores a single exponential relaxation process in the range of seconds was observed (Mauro, Nanavati & Heyer, 1972; Eisenberg *et al.*, 1973). The corresponding relaxation time showed an exponential increase with voltage and was attributed to the mean life-time of a pore. As outlined in part I (Boheim & Kolb, 1977) a second faster relaxation process in the range of milliseconds could be observed in addition. A likely explanation of the latter process was given on the basis of conductance changes caused by transients between adjacent pore states of a single pore. It was observed that the appearance of the faster relaxation process depends on the choice of experimental conditions under which the voltage-jump experiments were performed. Furthermore, it turned out that the absolute value of the slow relaxation time strongly varies with membrane pretreatment.

In general, the relaxation experiments do not yield information about the absolute values of conductance changes which are induced by the formation and disappearance of alamethicin pores and those arising from intrapore conductance fluctuations. As we will show in this paper more information may be obtained by correlation analysis which yields both the kinetic parameters of a multi-pore system and the absolute values of the corresponding conductance changes. The molecular mechanism of pore formation has not been completely elucidated as yet. Especially the behavior of alamethicin containing lipid bilayers in the range of weakly voltage-dependent conductance which was not accessible to relaxation studies as well as at very high levels of conductance are poorly understood. Besides the determination of all the parameters of the alamethicin-induced multi-pore state system we have drawn attention to these problems with the autocorrelation analysis.

Autocorrelation analysis has recently been introduced to study the ion transport mechanisms in lipid bilayers (Zingsheim & Neher, 1974; Kolb, Läuger & Bamberg, 1975; Moore & Neher, 1976; Kolb & Bamberg, 1977) and nerve membranes (Katz & Miledi, 1972; Anderson & Stevens, 1973; Conti, de Felice & Wanke, 1975; Fishman, Moore & Poussart, 1975). This method has the advantage that measurements of the autocorrelation function are carried out while the system is in an equilibrium or stationary state. It has been shown that in the case of gramicidin A-doped lipid

bilayers the autocorrelation analysis yields information both on the kinetic parameters of channel formation and the magnitude of the unit conductance step associated with the opening and closing of a channel. The results are in reasonable agreement with those of corresponding relaxation and single-channel experiments. The occurrence of a single correlation time could be explained on the basis of a simple two-state model of gramicidin A channel formation (Kolb *et al.*, 1975). For the well-established multi-state behavior of the alamethicin pore one should expect a more complex behavior of the autocorrelation function.

In the present paper we measured the autocorrelation function of alamethicin-doped lipid bilayers as a function of membrane voltage at different concentrations of alamethicin and electrolyte and different temperatures. The autocorrelation function could be described by a superposition of two single exponential functions of different correlation times. We will show that the two components of the autocorrelation function may be correlated to fluctuations in the number of pores and fluctuations between adjacent conductance states of individual pores, respectively.

Furthermore, we want to compare the amplitudes and correlation times obtained from the autocorrelation function with the corresponding values of the power spectral density. Recently, Wanke and Prestipino (1976) observed several time constants in the power density spectrum of conductance fluctuations produced by monazomycin-doped lipid membranes. The power spectral densities shown by Moore and Neher (1976) of monazomycin and alamethicin-doped lipid membranes also indicate that different time dependent processes may be involved in the mechanism of translocation of ions in these systems. On the basis of the Wiener-Khintchine theorem (Wiener, 1930; Khintchine, 1934) both methods, the autocorrelation and spectral analysis, should yield essentially the same information about the system under investigation. This agreement could be shown for gramicidin A-doped lipid membranes (Kolb & Bamberg, 1977). In this paper it will be shown that on the level of single-pore events of alamethicin-doped membranes the results of both methods are in close agreement. But on the basis of the autocorrelation analysis presented for multi-pore systems the corresponding spectral analysis yields a different amplitude especially for the slower process.

Materials and Methods

1,2-dioleoyl-sn-glycerol-3-phosphorylcholine (dioleoyllecithin) was synthetized and chromatographically purified in our laboratory by K. Janko. The pure R_F30 fraction of alamethicin was purchased from Microbiological Research Establishment, Porton Down/

Salisbury and checked by thin-layer chromatography. Alamethicin was added from an ethanolic/water (1 : 9 v/v) stock solution in amounts of 2.5 to 10 µg to 20 ml electrolyte solution. KCl salt solutions were 1 M, if not otherwise stated, and unbuffered (pH ≈ 5.5). KCl was p.A. grade from Merck. Black lipid membranes were formed in the usual way from a 1% (w/v) lipid solution in n-decane in a thermostated Teflon cell (Läuger, Lesslauer, Marti & Richter, 1967). The reproducibility of the temperature was within ±0.5 °C. The membrane area was between 6.5 and 7.2×10^{-3} cm^2. The area of the black film was determined by measuring the electrical capacitance of the film at low membrane voltage. For the specific capacitance of membranes made from dioleoylecithin a value of 0.38 µF/cm^2 (Stark, Benz, Pohl & Janko, 1972) was assumed. Single-pore experiments were carried out using Teflon cells with a hole of about 0.1 mm diameter.

Autocorrelation analysis of the membrane current noise was carried out under voltage clamp conditions as described previously (Kolb *et al.*, 1975; Kolb & Bamberg, 1977) using some minor modifications. The current was preamplified (Analog Devices Model 52 K) and passed through an eight-pole Butterworth filter (Krohn-Hite Model 3342). The feedback resistor was set to 5 MΩ and the feedback capacitor to 4 pF. The signal was then amplified by a dc-coupled amplifier (Princeton Applied Research Model 113). The output signal of the amplifier was usually stored on a magnetic-tape recorder (Precision Instruments Model 6200) with a frequency response from DC to 10 kHz. The stored signal was analyzed with a Honeywell-Saicor 43 A correlator. The processed autocorrelation function was recorded with an x−y recorder (Philips PM 8/25) and digitized by 100 to 200 points on a Hewlett-Packard 9864 A. The autocorrelation function was recorded at constant applied membrane voltage V. Each level of V was held constant for about 2–4 min. The time needed for a stable ac−dc uncoupling of the current noise depends on the high-pass filter position, but was usually less than 2 min. The autocorrelation function was computed during a time intervall of 50–90 sec. The autocorrelation function $\tilde{C}(\tau)$ of alamethicin-doped lipid membranes could be described by a linear superposition of two exponential functions and a constant offset C_∞ according to

$$\tilde{C}(\tau) = C(\tau) + C_\infty = C_f \cdot e^{-\tau/\tau_f} + C_s \cdot e^{-\tau/\tau_s} + C_\infty \tag{1}$$

where $C_0 = C(0)$ is the variance of the membrane current and τ_s, τ_f are the correlation times of the current. The offset C_∞ of the baseline depends mainly on the increase or decrease of the mean current during the sampling time of the correlator, but also on the high-pass filter position as described before. In nearly all cases C_∞ was found to be less than 5% of C_0.

The parameters C_∞, C_s, C_f, τ_s and τ_f given by Eq. (1) were evaluated in two different ways depending on the ratio $\tau_s/\tau_f (\tau_s > \tau_f)$. In case of $4\tau_f > \tau_s$ a single autocorrelation function was recorded and digitized. According to Eq. (1) the relation $\tilde{C}(\tau) \approx C_s \cdot \exp(-\tau/\tau_s) + C_\infty$ holds for correlation times τ well above a suitably chosen $\tau_c (\tau_f < \tau_c \lesssim \tau_s)$. The values of C_∞, C_s and τ_s were calculated by the method of least squares. The fit was optimized by varying τ_c. Thereafter the difference $(\tilde{C}(\tau) - C_s \cdot \exp(-\tau/\tau_s) - C_\infty)$ was fitted by the function $C_f \cdot \exp(-\tau/\tau_f)$. For the case $4\tau_f < \tau_s$ two autocorrelation functions were recorded for different time scales as shown in Fig. 1 *a*. As the Figure shows the time scale for the choice of the sample increment time of the correlator was adapted to the correlation times τ_s and τ_f to obtain an optimal record of the autocorrelation functions $C_s \cdot \exp(-\tau/\tau_s)$ and $C_f \cdot \exp(-\tau/\tau_f)$. Both functions were recorded from the same length of a record (50–90 sec) of the membrane current noise stored on the magnetic tape and fitted by an overall autocorrelation function according to Eq. (1). The corresponding parameters were determined by the method of least squares as described above. The result of the fit which corresponds to the autocorrelation function given in Fig. 1 *a* is shown in Fig. 1 *b*.

The filter positions of the bandfilter were adapted to the magnitude of the correlation times. The high-pass filter position was set to about $1/20\,\pi\,\tau_s$ and the low-pass filter position

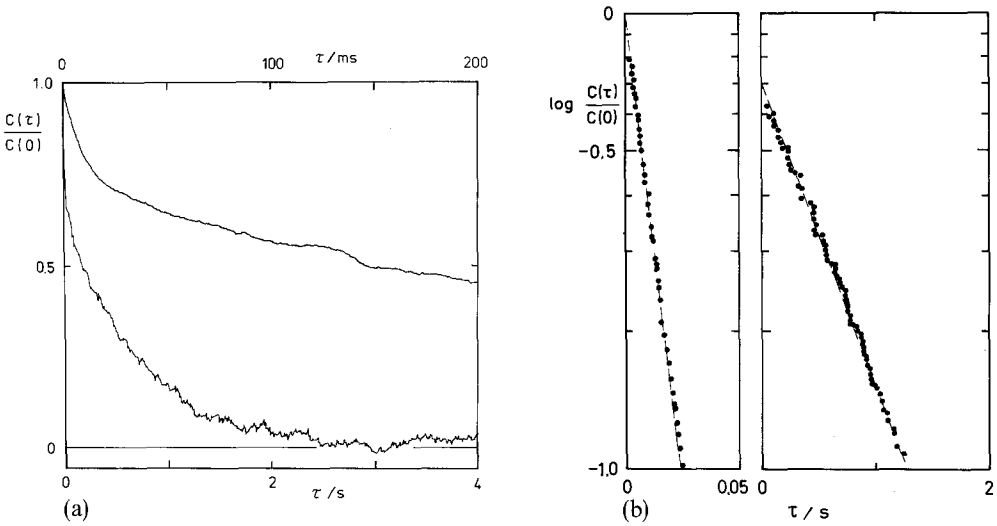

Fig. 1. (*a*) Autocorrelation function $C(\tau)$ of the current fluctuations divided by the initial value $C(0)=1.6\times10^{-18}$ A^2 versus time τ. For the upper trace the scale on the upper x-axis holds. Both functions were computed one after the other from the same record of current fluctuations of about equal length with a different choice of the sample increment of the autocorrelator. The lower trace contains 8192 summations, the upper 65,536. The mean membrane conductance was $\lambda_\infty=51$ μS cm^{-2}. Membrane area $A=7.1\times10^{-3}$ cm^2, external voltage $V=50$ mV. The aqueous phase contained 1 M KCl, 250 ng/cm^3 of alamethicin at 11 °C. (b) Logarithmic plot of $C(\tau)/C(0)$, as taken from Fig. 1 *a*, versus time for two different time ranges. The theoretical curve given by Eq. (1) was fitted by the method of least squares. For the amplitudes $C_s=1.1\times10^{-18}$ A^2 and $C_f=4.8\times10^{-19}$ A^2 were obtained and for the corresponding correlation times $\tau_s=0.65$ sec and $\tau_f=10.5$ msec. τ_s and τ_f are represented by the straight lines, respectively. The autocorrelation function was digitized by 150 points, part of them are outside the range of $C(\tau)/C(0)$ shown in the Figure

to about $10/\pi\tau_f$, respectively. The lowest high-pass filter position used was 0.01 Hz. For increasing correlation times τ_s up to about 5 sec (the longest correlation times measured in the present paper) the high-pass coupling frequency of 0.01 Hz induces an increasing distortion of the shape and amplitude of the autocorrelation function. This effect was described by De Felice and Sokol (1976) for a simple RC high-pass network. For the present paper the influence of the high-pass filter characteristics on τ_s and C_s was estimated as follows. The modification of a single exponential autocorrelation function induced by the used eight-pole Butterworth high-pass filter may be described by the relation (De Felice & Sokol, 1976):

$$C_n(\tau)=C_s\int_0^\infty \cos(2\pi f\tau)\cdot\frac{4\cdot\tau_s}{1+(2\pi f\cdot\tau_s)}\cdot g(f)\,df \tag{2}$$

where f denotes the frequency and $g(f)$ the frequency response of the high-pass filter. In the case of an n-pole Butterworth filter $g(f)$ may be described by the relation (Pregla & Schlosser, 1972):

$$g(f)=\frac{1}{1+\left(\frac{f_1}{f}\right)^{2\cdot n}}, \tag{3}$$

where n denotes the order of the pole of the filter and f_1 the high-pass filter position. The autocorrelation function given by Eqs. (2) and (3) was calculated by numerical integration using the method of Romberg quadrature (Ralston & Wilf, 1967) with the following choice of parameters: $f_1 = 0.01$ Hz, $C_s = 1$, $n = 8$ and $\tau_s = 5$ sec. If the numerically calculated function $C_n(\tau)$ is fitted by a single exponential function superimposed by an offset C_∞ the calculated values of τ_s and C_s differ by less than 2% from $C_s = 1$ and $\tau_s = 5$ sec. This fit was carried out for correlation times $\tau \lesssim 2 \cdot \tau_s$ as described previously (Kolb, Läuger & Bamberg, 1976). The small differences found for τ_s and C_s at $\tau_s = 5$ sec implies that the influence of high-pass filter position of 0.01 Hz is negligible under the conditions of our experiments.

Furthermore, experiments were carried out in which the membrane current noise was simultaneously processed by the correlator and a real time spectrum analyzer (Honeywell-Saicor-51 B) as described previously (Kolb & Bamberg, 1977) using some minor modifications. For the case of measurements of the power spectral density, the current noise was amplified in the same way as above. In order to obtain a low noise figure of the measurement circuit which was described in Kolb *et al.* (1975) the ratio of feedback resistance to source resistance was adjusted to about 10:1 (Poussart, 1971; Fishman, Poussart & Moore, 1975) in these experiments.

Results

The membrane conductance and the autocorrelation function of alamethicin-doped dioleoyllecithin/n-decane membranes were measured under a variety of conditions of temperature, alamethicin and electrolyte concentration. It is known that at a given membrane voltage the mean value of the membrane conductance strongly depends on the pretreatment of the membrane (Roy, 1975; Boheim & Kolb, 1977). Therefore, throughout the experiments we used a defined membrane pretreatment which is described in the following. For experiments which were performed at 30 and 25 °C the membrane was equilibrated for 90 min at that temperature. For measurements at lower temperatures the aqueous phase was held at 25 °C for 50 min and then cooled down to the desired temperature and equilibrated for another 40 min. After this equilibration in a zero voltage state the voltage was increased in steps of 5 mV and held constant at each level for 2–4 min. During this period both the stationary membrane conductance λ_∞ and the autocorrelation function were measured. If the membrane broke at high voltages (75–110 mV), further experiments were carried out using fresh aqueous solutions and following the procedure described above.

The Voltage-Conductance Relation

At first we describe the stationary properties of the membrane conductance at which the autocorrelation functions were recorded. Fig. 2

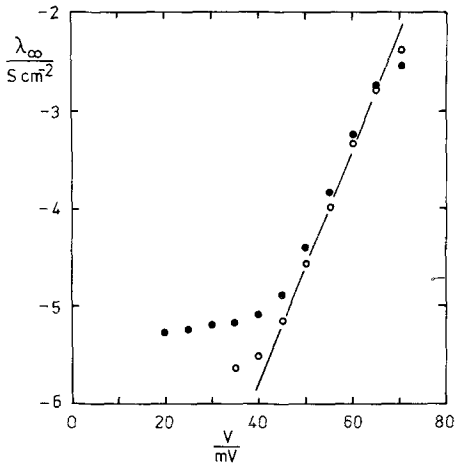

Fig. 2. Half-logarithmic plot of the mean membrane conductance λ_∞ versus voltage V. The measurements carried out in the first run are represented by the open circles. After the first series of experiments the stepwise record of the function $\lambda_\infty(V)$ was repeated as shown by the full circles. The straight line has been obtained by taking into account only the exponential voltage dependence of the conductance of the first run. The corresponding slope expressed in terms of $\alpha[\lambda_\infty]$ yields 6.8. The aqueous phase contained 1 M KCl and 250 ng/cm^3 alamethicin at 11 °C. For details *see text*

shows the typical stationary voltage-conductance relation $\lambda_\infty(V)$ of a given experiment. It may be seen from the figure that $\lambda_\infty(V)$ exhibits a weakly voltage-dependent characteristic at lower voltages followed by an exponential increase up to conductances of about 1 mS cm^{-2}. The values of λ_∞ represent mean values of the membrane conductance measured during the averaging time of the autocorrelator of about 50–90 sec. During this period one observes a more or less pronounced shift of the conductance to higher values at voltages which correspond to the range of weakly voltage-dependent conductance and a saturation of the conductance at high voltages in the range of $\lambda_\infty \geqq 1$ mS cm^{-2}. In both cases this shift could be estimated to be less than 10% of λ_∞. For intermediate voltages a similar shift of the conductance was not observed. In this voltage range the function $\lambda_\infty(V)$ could be described according to Mueller and Rudin (1968) and Eisenberg *et al.* (1973) by the relation:

$$\lambda_\infty(V) \sim \exp\{\alpha[\lambda_\infty] \cdot V \cdot F/RT\}^1. \tag{4}$$

Thus the slope of $\lambda_\infty(V)$ is expressed in terms of $\alpha[\lambda_\infty]$ and shows a significant increase with decreasing temperature (Table 1). The constant

1 The indices λ_∞, λ_s, τ_s, τ_f, etc. of the parameters α, δ and ε have been included in square brackets to obtain a clearer presentation. Functional dependences are indicated by round brackets as usual.

Table 1. Parameters of the voltage-conductance relation $\lambda_\infty(V)$ denoted by $\alpha[\lambda_\infty]$ and V_{100} as well as those of the correlation times τ_s and τ_f denoted by $\alpha^*[\tau_s]$, $\alpha^*[\tau_f]$, $\alpha[\tau_s]$, $\alpha[\tau_f]$ as a function of temperature[a]

	T(°C)			
	30	25	18	11
$\alpha[\lambda_\infty]$	5.8 ±0.3	6.0 ±0.4	6.5 ±0.2	6.8 ±0.3
V_{100}(mV)	51.2 ±6.5	50.1 ±5.8	54.4 ±5.1	53.5 ±3.9
$\alpha^*[\tau_s]$	0.39 ±0.03	0.48 ±0.03	0.51 ±0.02	0.58 ±0.02
$\alpha^*[\tau_f]$	0.036±0.003	0.040±0.004	0.046±0.003	0.047±0.004
$\alpha[\tau_s]$	2.3 ±0.3	2.8 ±0.2	3.3 ±0.2	3.9 ±0.3
$\alpha[\tau_f]$	0.22 ±0.05	0.24 ±0.04	0.30 ±0.04	0.35 ±0.05

[a] The voltage dependence is indicated by the parameters $\alpha[\lambda_\infty]$, $\alpha[\tau_s]$ and $\alpha[\tau_f]$, respectively; $\alpha^*[\tau_s]$ and $\alpha^*[\tau_f]$ indicate the conductance dependence of τ_s and τ_f, respectively. The voltage dependence of the different parameters was determined at a constant conductance of $\lambda_\infty = 100\ \mu S\ cm^{-2}$, the corresponding conductance dependence at a constant voltage of $V = 50$ mV. In addition V_{100} represents the voltage which corresponds to a membrane conductance of $\lambda_\infty = 100\ \mu S\ cm^{-2}$. Each value represents the mean ±SD. As membrane-forming solution dioleoyllecithin/*n*-decane was used. The aqueous phase contained 1 M KCl and 2.5×10^{-7} g/cm^3 alamethicin. For explanations *see text.*

Table 2. Parameters $\alpha[\lambda_\infty]$, $\alpha[\tau_s]$ and $\alpha[\tau_f]$ determining the voltage dependence of λ_∞, τ_s and τ_f, respectively, as well as the parameters $\alpha^*[\tau_s]$ and $\alpha^*[\tau_f]$ determining the conductance dependence of τ_s and τ_f as a function of the alamethicin concentration C_{AL}[a]

	C_{AL} (100 ng/cm^3)				
	5.0	3.75	3.25	2.5	1.25
$\alpha[\lambda_\infty]$	6.7 ±0.4	6.6 ±0.3	7.0 ±0.2	6.8 ±0.3	6.6 ±0.1
$\alpha^*[\tau_s]$	0.58 ±0.06	0.60 ±0.04	0.57 ±0.03	0.58 ±0.02	0.56 ±0.02
$\alpha^*[\tau_f]$	0.041±0.003	0.041±0.005	0.044±0.005	0.047±0.004	0.043±0.004
$\alpha[\tau_s]$	3.7 ±0.3	3.8 ±0.4	4.0 ±0.4	3.9 ±0.3	3.6 ±0.3
$\alpha[\tau_f]$	0.24 ±0.07	0.3 ±0.04	0.35 ±0.06	0.35 ±0.05	0.34 ±0.06

[a] The voltage dependence of the different parameters was determined at a constant conductance of $\lambda_\infty = 100\ \mu S\ cm^{-2}$, the corresponding conductance dependence at a constant voltage of $V = 50$ mV. Each value represents the mean ±SD. As membrane-forming solution dioleoyllecithin/*n*-decane was used; the aqueous phase contained 1 M KCl and was held at 11 °C. For further details *see text.*

of proportionality of Eq. (4) may be determined by specification of a voltage V_{100} which, when applied to the alamethicin-doped lipid membrane, induces a conductance of $100\ \mu S\ cm^{-2}$. As Table 1 indicates, V_{100} seems to be independent of temperature. If the membrane did not break at high conductances of about 3–5 mS cm^{-2} the measurement of the

Table 3. Parameter $\alpha[\lambda_\infty]$ determining the voltage dependence of λ_∞ and the parameters $\alpha^*[\tau_s]$ and $\alpha^*[\tau_f]$ characterizing the conductance dependence of τ_s and τ_f as a function of the ion concentration C_{KCl} [a]

	T(°C)	C_{KCl} (M)			
		1	0.5	0.25	0.1
$\alpha[\lambda_\infty]$	11	6.7 ±0.4	6.6 ±0.3	6.9 ±0.2	6.9 ±0.2
$\alpha[\lambda_\infty]$	25	5.8 ±0.3	5.8 ±0.3	6.0 ±0.2	5.9 ±0.3
$\alpha^*[\tau_s]$	11	0.58 ±0.03	0.56 ±0.02	0.56 ±0.04	0.6 ±0.03
$\alpha^*[\tau_s]$	25	0.46 ±0.04	0.49 ±0.04	0.47 ±0.06	0.47 ±0.05
$\alpha^*[\tau_f]$	11	0.043±0.006	0.046±0.01	0.046±0.008	0.044±0.006
$\alpha^*[\tau_f]$	25	0.041±0.006	0.040±0.01	0.035±0.003	0.031±0.006

[a] The voltage dependence of λ_∞ was determined at a constant conductance of $\lambda_\infty = 100\,\mu S\,cm^{-2}$, the conductance dependence of τ_s and τ_f at a constant voltage of $V = 50$ mV. Each value represents the mean ±SD. As membrane-forming solution dioleoyllecithin/n-decane was used; the aqueous phase contained 500 ng/cm^3 alamethicin. The temperature was held at 11 °C and 25 °C, respectively. For details *see text*.

function $\lambda_\infty(V)$ was repeated at the same membrane. Before the new record was started the voltage was set to zero for about 20 min. During these experiments the weakly voltage-dependent conductance increased from about 1 $\mu S\,cm^{-2}$ up to 60 $\mu S\,cm^{-2}$; sometimes V_{100} shifted up to 10 mV to lower values and the saturation behavior of $\lambda_\infty(V)$ started at about 3–10 mV lower voltages (*see also* Fig. 2). As a consequence of this variation of $\lambda_\infty(V)$ the slope $\alpha[\lambda_\infty]$ decreased up to 4% which lies within the experimental error of $\alpha[\lambda_\infty]$ (Table 1). If the function $\lambda_\infty(V)$ was measured first at 11 °C and then recorded again at 25 °C on the same membrane, the weakly voltage-dependent conductance increased up to 200 $\mu S\,cm^{-2}$. Because we want to compare measurements obtained under similar conditions of weakly voltage-dependent conductance, these results were discarded. A similar increase of the weakly voltage-dependent conductance was not observed if the experiment was first performed at the higher temperature.

As may be seen from Table 2, $\alpha[\lambda_\infty]$ seems to be independent of the alamethicin concentration C_{AL}. Furthermore, a change of the ion concentration C_{KCl} in the range of 0.1 to 1 M KCl does not influence $\alpha[\lambda_\infty]$ (Table 3), whereas λ_∞ varies considerably. In agreement with Mueller and Rudin (1968) and Eisenberg *et al.* (1973) we found that at constant voltage and temperature the dependence of λ_∞ on C_{AL} and C_{KCl} could be described

in terms of:

$$\lambda_\infty \sim C_{AL}{}^{\delta[\lambda_\infty]} \cdot C_{KCl}{}^{\varepsilon[\lambda_\infty]}, \quad (V,\ T = \text{const.}). \tag{5}$$

Fig. 3*a* shows the plot $\log \lambda_\infty$ *vs.* C_{AL} at a constant voltage of 50 mV, 1 M KCl and 11 °C. The straight line yields $\delta[\lambda_\infty] = 9.8$. The temperature dependence of $\delta[\lambda_\infty]$ was not investigated. Measurements of λ_∞ with varing ion concentration in the range of 0.1 to 1 M KCl at different temperatures indicate a slight increase of the corresponding slope $\varepsilon[\lambda_\infty]$ with decreasing temperature (Fig. 3*b*). The straight lines drawn in Fig. 3*b* yield $\varepsilon[\lambda_\infty] = 5.8$ at 25 °C and $\varepsilon[\lambda_\infty] = 7.9$ at 11 °C.

The Autocorrelation Function

The autocorrelation functions of alamethicin-induced current noise in lipid membranes were measured with increasing membrane voltage. At mean membrane conductances $\lambda_\infty \geqq 100$ nS cm^{-2} the autocorrelation function could be fitted by a linear superposition of two exponential functions. A typical record is presented in Fig. 1*a*. The fit of the autocorrelation function according to Eq. (1) was carried out by the method of least squares. Fig. 1*b* shows the fit of the autocorrelation function given in Fig. 1*a*. The result indicates that the shape of the autocorrelation function is characterized by two different time constants. It turned out that the shape and amplitude of the autocorrelation function are more reproducible functions of the mean conductance λ_∞ than of the membrane voltage. The significance of this finding will be discussed later.

The Correlation Times

Fig. 4*a* shows the slow correlation time τ_s and the fast correlation time τ_f of a single membrane as a function of λ_∞ at $C_{AL} = 250$ ng/cm^3, 1 M KCl and 11 °C. Both correlation times increase up to one order of magnitude in the range of weakly voltage-dependent conductance and level off to a linear behavior (on the logarithmic scale) for voltage-dependent conductances. The corresponding slopes of the linear portion of the curves are quite different which indicates a strong dependence of τ_s on λ_∞ whereas τ_f remains nearly constant. If these slopes are described in terms of $\alpha^*[\tau_s]$ and $\alpha^*[\tau_f]$ according to the relation

$$\tau_{s,\,f}(\lambda_\infty) \sim (\lambda_\infty)^{\alpha^*[\tau_{s,\,f}]} \quad (T = \text{const.}) \tag{6}$$

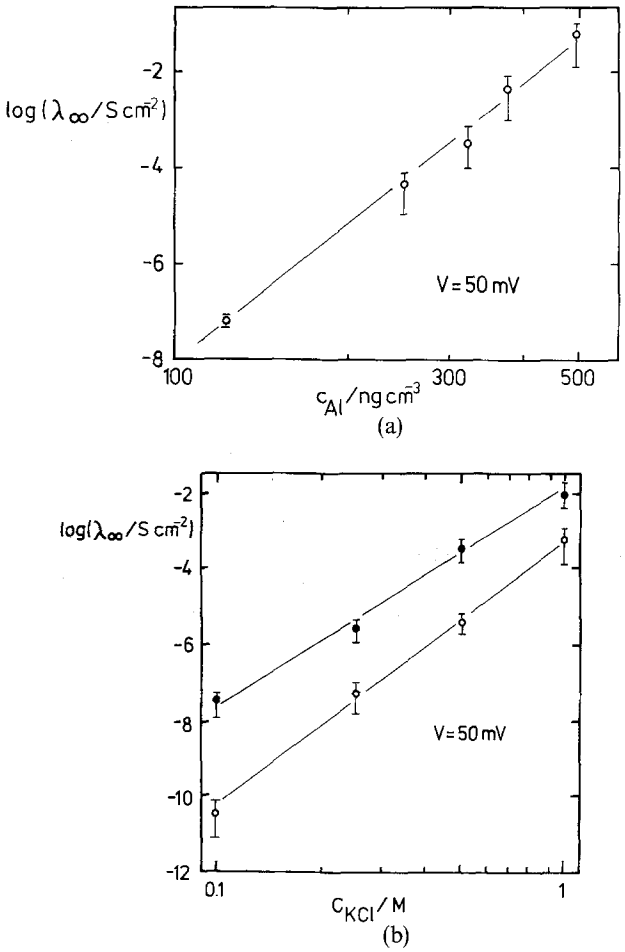

Fig. 3. (*a*) Dependence of the mean membrane conductance λ_∞ on the alamethicin concentration C_{AL} at constant voltage $V=50$ mV; 1 M KCl and 11 °C. Each point represents the mean value of five experiments, the bars indicating the standard deviation. According to Eq. (5) the straight line yields $\delta[\lambda_\infty]=9.8$. (b) Dependence of the mean membrane conductance λ_∞ on the concentration of KCl (C_{KCl}) at constant voltage $V=50$ mV for the following temperatures: ●, 11 °C, ○, 25 °C. The aqueous phase contained 500 ng/cm³ alamethicin. Each point represents the mean value ± SD of five experiments. According to Eq. (5) the straight lines yield $\varepsilon[\lambda_\infty]=5.8$ and $\varepsilon[\lambda_\infty]=7.9$ at 25 and 11 °C, respectively

one finds for the straight lines shown in Fig. 4*a* $\alpha^*[\tau_s]=0.57$ and $\alpha^*[\tau_f]=0.049$. At high conductances ($\lambda_\infty \geqq 1$ mS cm^{-2}) τ_s bends off to approach a constant level. The temperature dependence of τ_s and τ_f is presented in Fig. 4*b*. For the sake of a clearer presentation the values of τ_s and τ_f connected with the weakly voltage-dependent conductance were

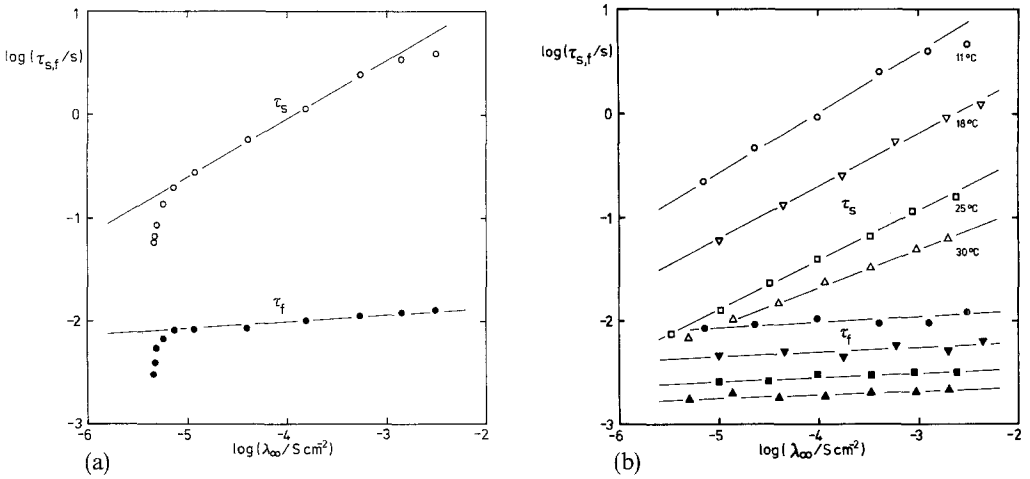

Fig. 4. (*a*) Slow correlation time τ_s (open circles) and fast correlation time τ_f (full circles) versus mean membrane conductance λ_∞. The experimental points represent measurements on a single membrane. The aqueous phase contained 1 M KCl, 250 ng/cm^3 alamethicin at 11 °C. According to Eq. (6) the straight lines represent the following values: $\alpha^*[\tau_s]=0.57$ and $\alpha^*[\tau_f]=0.049$. (*b*) Slow correlation time τ_s (open symbols) and fast correlation time τ_f (full symbols) versus mean membrane conductance λ_∞. The experimental points were obtained from different membranes at the following temperatures: △, ▲, 30 °C; □, ■, 25 °C; ▽, ▼, 18 °C; ○, ●, 11 °C. For the sake of a clearer presentation the results obtained for the range of weakly voltage-dependent conductance (shown in Fig. 4*a*) were omitted. According to Eq. (6) the straight lines represent the following slopes: $\alpha^*[\tau_s]=0.37$, $\alpha^*[\tau_f]=0.035$ at 30 °C; $\alpha^*[\tau_s]=0.49$, $\alpha^*[\tau_f]=0.042$ at 25 °C; $\alpha^*[\tau_s]=0.51$, $\alpha^*[\tau_f]=0.048$ at 18 °C; $\alpha^*[\tau_s]=0.58$, $\alpha^*[\tau_f]=0.047$ at 11 °C. The aqueous phase contained 1 M KCl and 250 ng/cm^3 alamethicin

omitted. At constant λ_∞ both correlation times increase with decreasing temperature, but as the straight lines in Fig. 4*b* indicate the corresponding slopes $\alpha^*[\tau_s]$ and $\alpha^*[\tau_f]$ vary differently. $\alpha^*[\tau_s]$ increases from 0.37 to 0.58 for a temperature reduction from 30 to 11 °C whereas $\alpha^*[\tau_f]$ remains nearly constant at a value of $\alpha^*[\tau_f]\approx 0.04$. As may be seen from Table 1, $\alpha^*[\tau_s]$ and $\alpha^*[\tau_f]$ are only slightly different from membrane to membrane. Even variations of the voltage-conductance characteristics as described above have no significant influence either on the slopes or on the absolute values of τ_s and τ_f *at constant conductance* λ_∞. Due to the temperature-independent behavior of $\alpha^*[\tau_f]$ the activation energy $E_A(\tau_f)$ of the fast correlation time could be determined independent of λ_∞ within the range of voltage-dependent conductance; we obtained $E_A(\tau_f)\approx 12$ kcal/mol. The activation energy $E_A(\tau_s)$ of the slow correlation process changes with conductance (Fig. 4*b*); at a moderate conductance of 100 μS cm^{-2} one finds $E_A(\tau_s)\approx 49$ kcal/mol.

For comparison with the corresponding results of part I (Boheim & Kolb, 1977) τ_s and τ_f were also plotted as functions of voltage. In the range of voltage-dependent conductance the slopes of τ_s and τ_f versus voltage could be described in terms of $\alpha[\tau_s]$ and $\alpha[\tau_f]$ according to the relation

$$\tau_{s,f}(V) \sim \exp\{\alpha[\tau_{s,f}] \cdot V \cdot F/RT\}. \tag{7}$$

The experimental values of $\alpha[\tau_s]$ and $\alpha[\tau_f]$ are summarized in Table 1. From Eqs. (1), (6) and (7) one finds that $\alpha[\tau_{s,f}]$ and $\alpha^*[\tau_{s,f}]$ are connected by the relation:

$$\alpha[\tau_{s,f}] = \alpha^*[\tau_{s,f}] \cdot \alpha[\lambda_\infty]. \tag{8}$$

Using the values of $\alpha^*[\tau_{s,f}]$, $\alpha[\lambda_\infty]$ and $\alpha[\tau_{s,f}]$ given in Table 1 it may be easily verified that the experimentally determined values of $\alpha[\tau_{s,f}]$ are in close agreement with those calculated from Eq. (8).

For a change of the alamethicin concentration in the range 125 to 500 ng/cm^3 $\alpha^*[\tau_s]$, $\alpha^*[\tau_f]$ as well as $\alpha[\tau_s]$ and $\alpha[\tau_f]$ remain unchanged (Table 2). On the other hand, the absolute values of τ_s and τ_f behave differently whether the applied voltage or the mean membrane conductance are held constant. At constant voltage the slow correlation time increases with increasing alamethicin concentration, whereas τ_f remains nearly constant. This behavior could be described by the relation:

$$\tau_{s,f} \sim C_{\mathrm{AL}}{}^{\delta[\tau_{s,f}]} \quad (V,\ T = \text{const.}). \tag{9}$$

Fig. 5*a* shows the plot of $\log\tau_s$ *vs.* C_{AL} and of $\log\tau_f$ *vs.* C_{AL} at a constant voltage of 50 mV and 11 °C. The values of τ_s and τ_f were partly determined by extrapolation. For the slope of the straight lines given in Fig. 5*a* one finds $\delta[\tau_s] = 4.2$ and $\delta[\tau_f] \approx 0$. At constant conductance λ_∞, however, the quantities τ_s and τ_f appear to be nearly independent of alamethicin concentration (Fig. 5*b*). Comparison of the experimental errors of the slow correlation times τ_s presented in Figs. 5*a* and 5*b* show that τ_s is a more reproducible function of conductance than of the applied voltage. In case of τ_f both representations yield essentially the same experimental error.

The variations of τ_s and τ_f with changing electrolyte concentration C_{KCl} and those of their corresponding slopes $\alpha[\tau_s]$, $\alpha[\tau_f]$, $\alpha^*[\tau_s]$, $\alpha^*[\tau_f]$ are similar to the variations of these parameters with changing alamethicin concentration. $\alpha^*[\tau_s]$ and $\alpha^*[\tau_f]$ show no significant dependence on C_{KCl} in the range of 0.1 to 1 M. This is also valid for $\alpha[\tau_s]$ and $\alpha[\tau_f]$ which may be seen from Eq. (8) using the corresponding values of $\alpha[\lambda_\infty]$, $\alpha^*[\tau_s]$ and

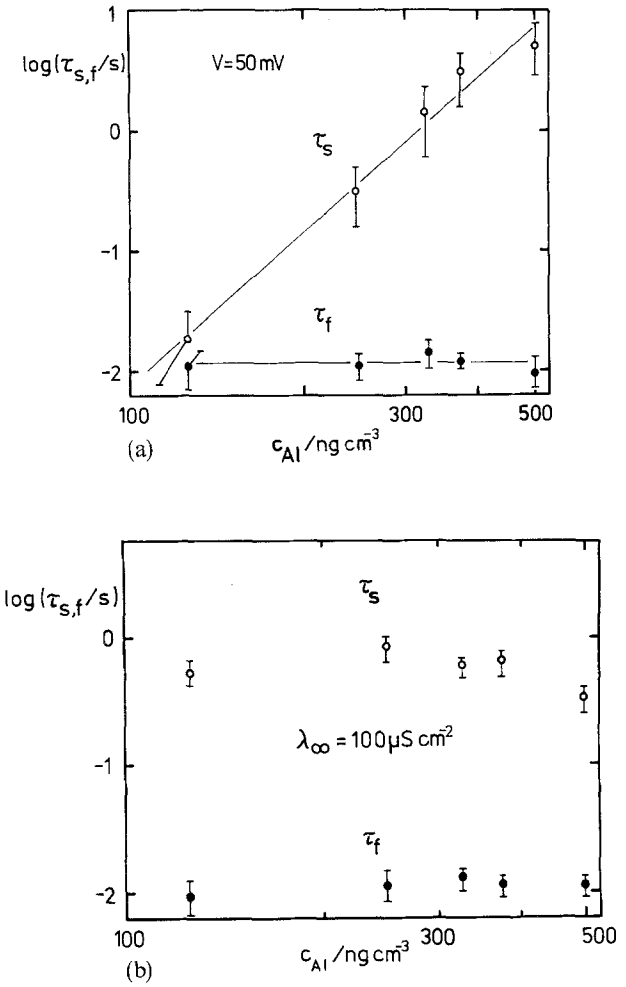

Fig. 5. (*a*) Slow correlation time τ_s (open circles) and fast correlation time τ_f (full circles) as a function of alamethicin concentration C_{AL} at constant voltage $V=50$ mV; 1 M KCl and 11 °C. Each point represents the mean value ±SD. According to Eq. (9) the straight lines represent the following slopes: $\delta[\tau_s]=4.2$ and $\delta[\tau_f]=0$. (*b*) Slow correlation time τ_s (open circles) and fast correlation time τ_f (full circles) as a function of alamethicin concentration C_{AL} at constant mean membrane conductance $\lambda_\infty=100\,\mu S\,cm^{-2}$; 1 M KCl and 11 °C. The data were taken according to the experiments of Fig. 5*a*

$\alpha^*[\tau_f]$ given in Table 3. At constant voltage the absolute values of τ_s decrease with decreasing C_{KCl}, whereas τ_f remains constant within experimental error. From Fig. 6*a* it may be seen that the correlation time τ_s approximately follows the relation

$$\tau_s \sim C_{KCl}^{\varepsilon[\tau_s]} \quad (V,\ T=\text{const.}) \tag{10}$$

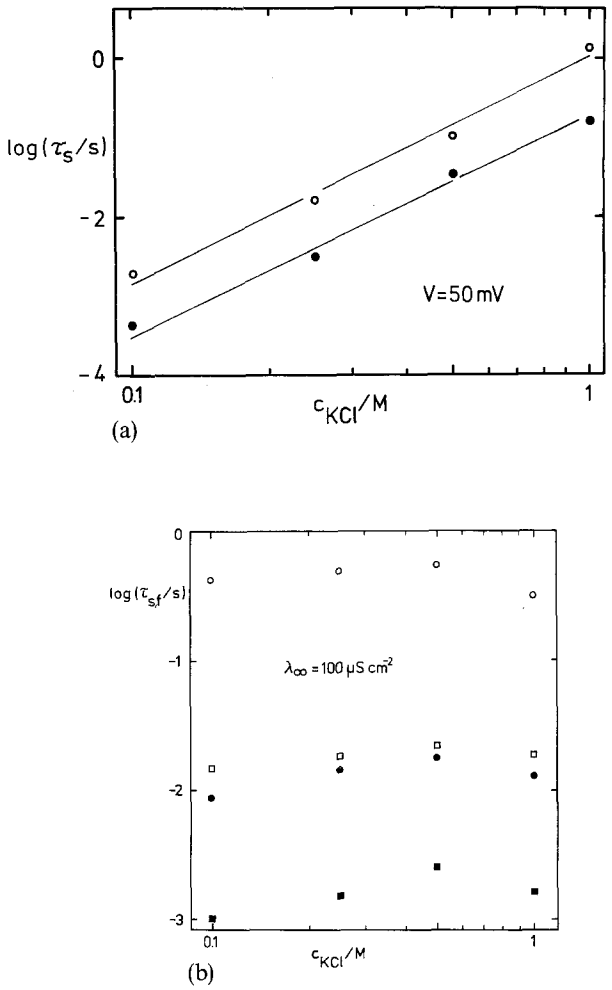

Fig. 6. (*a*) Slow correlation time τ_s as a function of ion concentration C_{KCL} at constant applied voltage $V=50$ mV and an alamethicin concentration $C_{AL}=500$ ng/cm^3; in the experiments at 25 °C and with $C_{KCL}=0.1$ M an alamethicin concentration of 1 μg/cm^3 was used. Open circles refer to 11 °C, full circles to 25 °C. According to Eq. (10) the straight lines represent the following slopes: $\varepsilon[\tau_s]=2.8$ at 11 °C and $\varepsilon[\tau_s]=2.6$ at 25 °C. (*b*) Correlation times τ_s (open symbols) and τ_f (full symbols) as a function of ion concentration C_{KCl} at constant mean membrane conductance $\lambda_\infty=100$ μS cm^{-2} and at an alamethicin concentration $C_{AL}=500$ ng/cm^3. Circles refer to 11 °C, squares to 25 °C

which is analogous to Eq. (9). The straight lines plotted in Fig. 6*a* yield $\varepsilon[\tau_s]=2.8$ at 11 °C and $\varepsilon[\tau_s]=2.6$ at 25 °C. At constant membrane conductance, however, τ_s and τ_f remain virtually constant for a concentration change from 0.1 to 1 M KCl (Fig. 6*b*).

The Correlation Amplitudes

Under voltage clamp conditions the current J is found to fluctuate in time t around a mean value $\bar{J}$:

$$J(t) = \bar{J} + \delta J(t).$$

The corresponding autocorrelation function of $\delta J(t)$ is defined according to the relation:

$$C(\tau) = \overline{\delta J(t) \cdot \delta J(t+\tau)}. \tag{11}$$

The variance of the current is given by:

$$C(0) = \overline{(\delta J)^2} = \sigma_J{}^2. \tag{12}$$

In case of voltage-clamp experiments the variance of conductance fluctuations is obtained as:

$$C^*(0) \equiv \sigma_\lambda{}^2 = \frac{1}{V^2} \cdot \sigma_J{}^2 \tag{13}$$

where λ is the macroscopic conductance expressed in S. Figs. 1*a* and 1*b* indicate that $\sigma_\lambda{}^2$ contains two components which seem to arise from two different sources of conductance fluctuations. These two components differ in their dependence on temperature and mean conductance λ_∞ as shown in the previous section. Due to the different time scales of the fast and the slow process as shown in the previous section the corresponding current fluctuations can be measured separately by selecting appropriate filters. The superposition of the autocorrelation function of the fast and slow process obtained by this procedure should yield the same result as obtained from Eq. (1). This method of evaluation has been carried out as an additional check for a fit of the autocorrelation function of the broad-band amplified current fluctuations by applying Eq. (1) as follows. The autocorrelation function of a record of $\delta J(t)$ of given length was processed in two different ways. First the amplitudes C_s and C_f of $C(\tau)$ [Eq. (1)] were determined as usual from the autocorrelation analysis of the membrane current using a broad-band amplifier. Then C_s and C_f were separately determined from the same part of the record. For this purpose the broad-band amplified current was additionally filtered by a narrow-band filter. The corresponding filter positions were set to $0.1 \cdot \tau_s \lesssim \tau_s \lesssim 5 \cdot \tau_s$ and $5 \cdot \tau_f \gtrsim \tau_f \gtrsim 10^{-4}$ sec, respectively. In both cases the output of the filter could be fitted by an autocorrelation function of single exponential

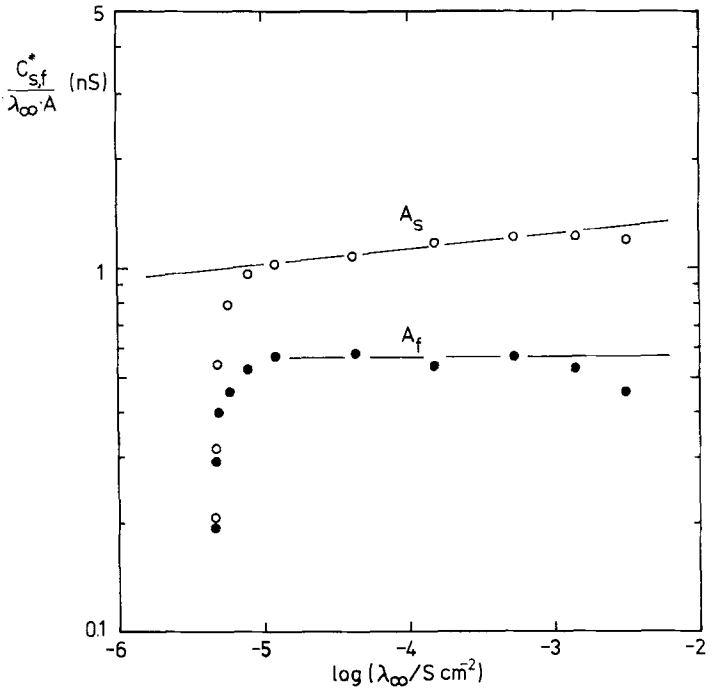

Fig. 7. $C_s^*/\lambda_\infty \cdot A$ (open circles) and $C_f^*/\lambda_\infty \cdot A$ (full circles) as a function of mean membrane conductance λ_∞. A is the membrane area. The points have been calculated from the experiment of Fig. 4*a*. The aqueous phase contained 1 M KCl, 250 ng/cm^3 alamethicin at 11 °C. According to Eq. (15) the straight lines represent the following slopes: $\alpha^*[A_s]=0.07$ and $\alpha^*[A_f]=0$

behavior of amplitude C_s and C_f, respectively. In both cases the values obtained for C_s and C_f agreed within an error of 5% which confirms the formulation of the autocorrelation function given by Eq. (1). Fig. 7 shows the parameters $C^*_{s,f}/\lambda_\infty \cdot A$, where A denotes the membrane area of a single membrane, as function of conductance λ_∞ at 1 M KCl and and 11 °C. C_s^* and C_f^* denote the correlation amplitudes of conductance fluctuations which are related to the corresponding correlation amplitudes of current fluctuations according to Eq. (13). In the following we use the abbreviation:

$$A_{s,f} = \frac{C^*_{s,f}}{\lambda_\infty \cdot A}. \tag{14}$$

Both parameters increase strongly with λ_∞ in the range of the weakly voltage-dependent conductance and bend off in the range where the voltage-dependent conductance appears. At high conductances $\lambda_\infty \gtrsim 1$ mS cm^{-2}, A_s shows a saturation behavior similar to that observed

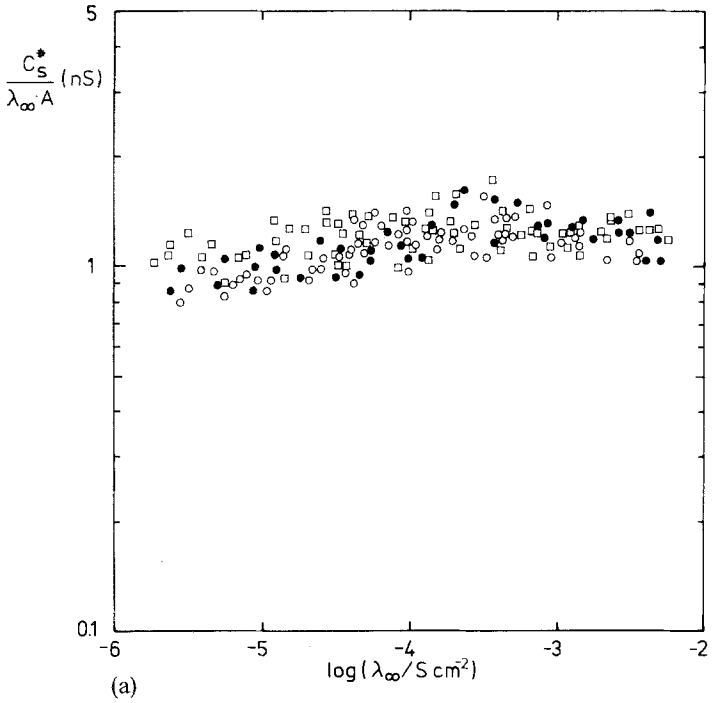
5
1
0.1
$\frac{C_s^*}{\lambda_\infty \cdot A}$ (nS)
-6
-5
-4
-3
-2
log (λ_∞/S cm^{-2})

(a)

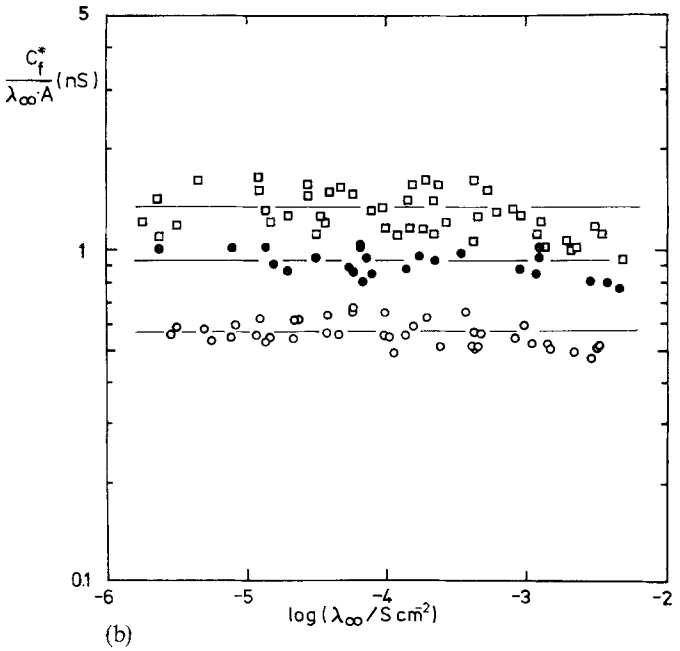
5
1
0.1
$\frac{C_f^*}{\lambda_\infty \cdot A}$ (nS)
-6
-5
-4
-3
-2
log (λ_∞/S cm^{-2})

(b)

for τ_s (Fig. 4*a*), A_f decreases significantly, whereas τ_f remains unchanged as shown in the previous section. As Fig. 7 shows, the linear behavior of A_s and A_f *vs.* $\log \lambda_\infty$ may be described for the range of voltage-dependent conductance up to $\lambda_\infty \approx 1$ mS cm^{-2} by the relation:

$$A_{s,f} \sim \lambda_\infty^{\alpha^*[A_{s,f}]} \quad (T = \text{const.}). \tag{15}$$

The straight lines in Fig. 7 were drawn using the values $\alpha^*[A_s] = 0.07$ and $\alpha^*[A_f] \simeq 0$. For the further considerations we restrict ourselves to this range of voltage-dependent conductance. It may be seen from the comparison of Figs. 8*a* and 8*b* that A_s and A_f exhibit a quite different temperature dependence; A_f increases with increasing temperature, whereas A_s remains virtually constant. The activation energy $E_A(A_f)$ of A_f yields $E_A(A_f) \approx 10.5$ kcal/mol. Comparison of the experimental values of A_s obtained at a single membrane (Fig. 7) with the corresponding values obtained from different membranes (Fig. 8*a*) shows the scatter of A_s. Scatter of similar magnitude was observed for A_s plotted as a function of voltage. $\alpha^*[A_s]$ and $\alpha^*[A_f]$ were determined separately for each experiment and found to be independent of temperature; mean values of $\alpha^*[A_s] = 0.08 \pm 0.03$ and $\alpha^*[A_f] \approx 0$ are obtained. In analogy to Eq. (7) we denote the parameter describing the voltage dependence of A_s by $\alpha(A_s)$. From a plot A_s *vs.* V we found $\alpha[A_s] = 0.45 \pm 0.1$, independent of temperature.

Within experimental error an influence of the alamethicin concentration on the absolute values of A_s at constant conductance as well as on $\alpha^*[A_s]$ and $\alpha[A_s]$ could not be detected; the same was found for A_f and $\alpha^*[A_f]$ and also $\alpha[A_f]$. Upon decreasing the ion concentration the amplitudes of the autocorrelation function were found to decrease on the average

Fig. 8. (*a*) $C_s^*/\lambda_\infty \cdot A$ as a function of mean membrane conductance λ_∞ at different temperatures: ○, 11 °C; ●, 18 °C; □, 25 °C. A denotes the membrane area. The conductance λ_∞ was varied by varying the applied voltage. For sake of a clearer presentation the results obtained in the range of weakly voltage-dependent conductance were omitted. At each temperature between four and six different membranes were used for the measurements. The aqueous phase contained 1 M KCl and 250 ng/cm^3 alamethicin. (*b*) $C_f^*/\lambda_\infty \cdot A$ as a function of mean membrane conductance λ_∞ at different temperatures: ○, 11 °C; ●, 18 °C; □, 25 °C. Experimental conditions were the same as described for Fig. 8*a*

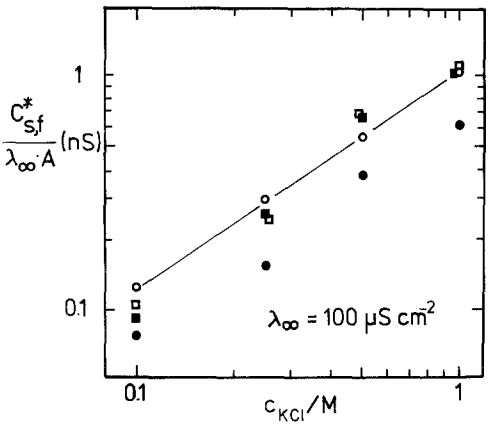

Fig. 9. $C^*_s/\lambda_\infty \cdot A$ (open symbols) and $C^*_f/\lambda_\infty \cdot A$ (full symbols) as a function of ion concentration C_{KCl} at constant mean membrane conductance $\lambda_\infty = 100\,\mu S\,cm^{-2}$ and alamethicin concentration of 500 ng/cm^3. A denotes the membrane area. Experiments carried out at 11 °C are denoted by circles and at 25 °C by squares. According to Eq. (16) the slope of the straight line yields $\varepsilon[A_s] = 0.8$

proportional to the weakly voltage-dependent conductance. In the range of voltage-dependent conductance both A_s and A_f decrease to the same extent. According to Fig. 9 this behavior of A_s and A_f may be described at constant conductance by the relation:

$$A_{s,f} \sim C_{KCl}^{\varepsilon[A_s,f]} \quad (\lambda_\infty = \text{const.}). \tag{16}$$

As the Figure shows there is no significant difference between $\varepsilon[A_s]$ and $\varepsilon[A_f]$. The straight lines in Fig. 9 were drawn according to $\varepsilon[A_{s,f}] = 0.8$.

Power Spectral Density

Measurements of the power spectral density of the current noise were performed in addition to the autocorrelation analysis. Both quantities, the autocorrelation function and the power spectral density are correlated by the Wiener-Khintchine transformation (Wiener, 1930; Khintchine, 1934) and yield essentially the same information. In this way, the correlation times and amplitudes may be obtained by a second independent, experimental method. Power density measurements may therefore be used as an additional check that the autocorrelation function $C(\tau)$ [*see* Eq. (1)] may

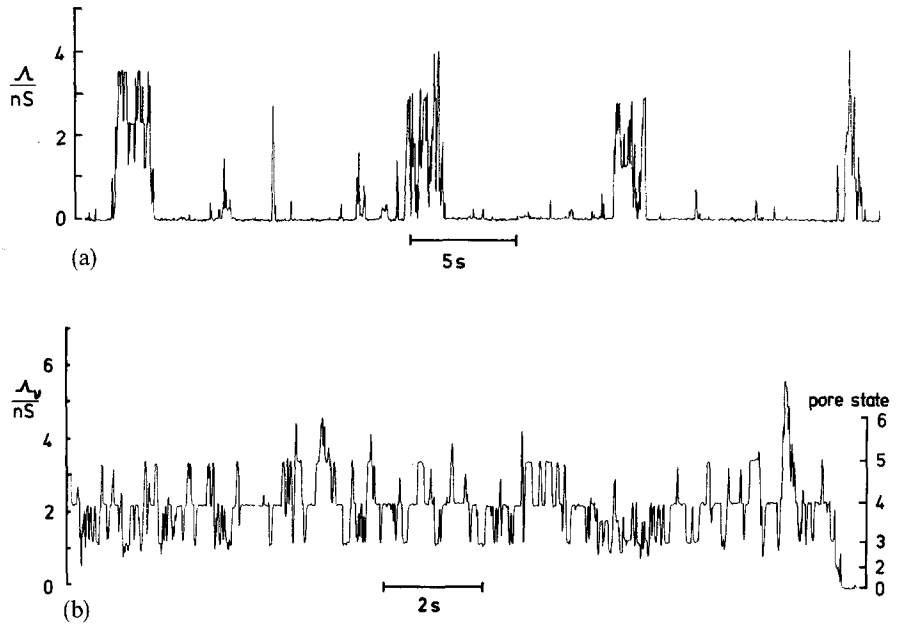

Fig. 10. (*a*) Conductance fluctuations of an alamethicin-doped black lipid membrane versus time t in the presence of single conducting pores (bursts). The membrane-forming solution was 1% dioleoyllecithin in *n*-decane. The aqueous phase contained 1 M KCl and a nominal alamethicin concentration of 50 ng/cm^3 at 4 °C. The applied voltage was 130 mV. (*b*) Conductance fluctuations Λ_ν of an alamethicin-doped black lipid membrane versus time t of *one* conducting pore at 4 °C and an applied voltage of 120 mV. The scale on the right denotes the corresponding pore states ν. Experimental conditions were the same as described for Fig. 10*a*

be described by a superposition of two separate single exponential functions. The power spectral density of the autocorrelation function given by Eq. (1) may be calculated from the Wiener-Khintchine transformation of $C(\tau)$ yielding a superposition of two Lorentzian curves:

$$S(f)=\frac{4\cdot\tau_s\cdot C_s}{1+(2\pi\tau_s\cdot f)^2}+\frac{4\cdot\tau_f\cdot C_f}{1+(2\pi\tau_f\cdot f)^2}, \tag{17}$$

where C_s, C_f and τ_s, τ_f are the parameters of the corresponding autocorrelation function described in Eq. (1).

As additional support for the assignment of the parameters obtained by autocorrelation analysis and power spectral density from multi-pore systems of alamethicin-doped lipid membranes to single-pore parameters, which is outlined in the Discussion, we also performed autocorrelation analysis and power spectral density measurements on single-pore systems. Fig. 10*a* shows a part of a typical record of conductance fluctuations

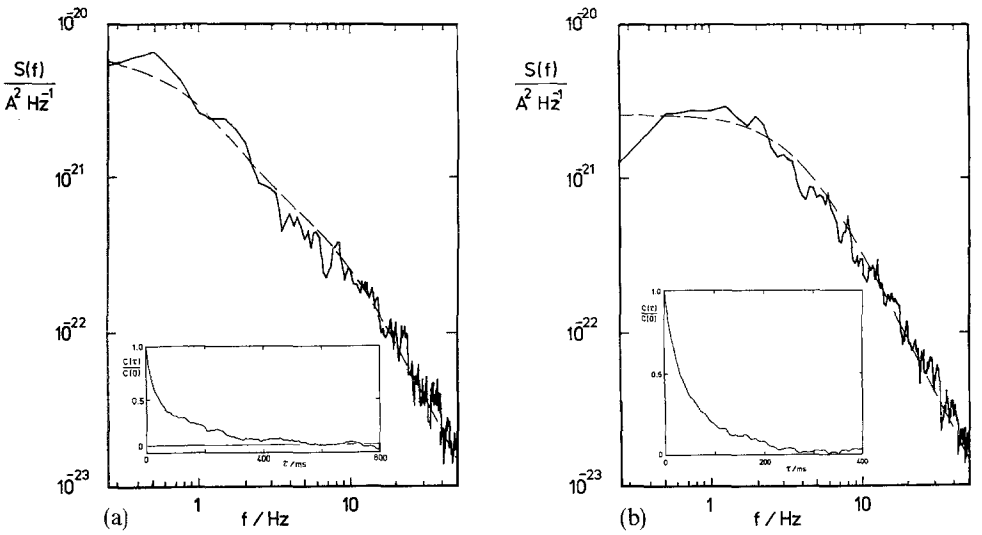

Fig. 11. (*a*) Power spectral density $S(f)$ of current fluctuations induced by single conducting pores versus frequency f. Part of the corresponding conductance fluctuations are shown in Fig. 10*a*. The power spectral density shown is an average of 16 spectra. The theoretical curve was drawn according to Eq. (17) using the values $C_s = 8.2 \times 10^{-21}$ A^2, $C_f = 6.9 \times 10^{-21}$ A^2, $\tau_s = 190$ msec and $\tau_f = 21$ msec determined by the simultaneously processed autocorrelation function $C(\tau)$ shown in the inset. For further explanations *see text. Inset:* Autocorrelation function $C(\tau)$ of the current fluctuations induced by single conducting pores divided by the initial value $C(0) = 1.51 \times 10^{-20}$ A^2 versus time τ. The autocorrelation function shown is an average of 65,536 summations. This analysis was done on data processed through a high-pass filter of 0.03 Hz. Experimental conditions were the same as described for Fig. 10*a*. (*b*) Power spectral density $S(f)$ of current fluctuations induced by *one* conducting pore versus frequency f. Part of the corresponding conductance fluctuations are shown in Fig. 10*b*. The power spectral density shown is an average of 16 spectra. The processing of $S(f)$ was completed before the pore switched to the nonconducting state seen at the right end of the record of conductance fluctuations shown in Fig. 10*b*. The theoretical curve was drawn according to Eq. (17), using the values $C_s = 0$, $C_f = 1.5 \times 10^{-20}$ A^2 and $\tau_f = 44$ msec determined by the simultaneously processed autocorrelation function $C(\tau)$ shown in the inset. For further explanations *see text. Inset:* Autocorrelation function $C(\tau)$ divided by the initial value $C(0) = 1.5 \times 10^{-20}$ A^2 versus time τ. The autocorrelation function shown is an average of 32,768 summations. This analysis was done on data processed through a high-pass filter of 0.03 Hz. Experimental conditions were the same as described for Fig. 10*b*

arising from single alamethicin pores (bursts) at 4 °C, 1 M KCl and an applied voltage of $V = 130$ mV. The power spectral density $S(f)$ (Fig. 11*a*) and autocorrelation function (inset of Fig. 11*a*) of the corresponding current fluctuations show two processes of different time behavior. The theoretical curve following the trace of $S(f)$ was calculated from Eq. (17) using the parameters $C_s = 8.2 \times 10^{-21}$ A^2, $C_f = 6.9 \times 10^{-21}$ A^2 and $\tau_s = 190$ msec, $\tau_f = 21$ msec determined from the simultaneously processed

Table 4. Parameters of a single fluctuating pore in a 1% dioleoyl/*n*-decane membrane at 4 °C, $V=120$ mV, 1 M KCl and in the presence of nominal 50 ng/cm^3 alamethicin R_F30[a]

v	p_v (%)	τ_v (msec)	Λ_v (nS)
2	3.0	29	0.57
3	29.4	45	1.29
4	51.7	69	2.36
5	14.7	43	3.50
6	1.2	23	4.71

[a] v denotes the pore state and p_v the probability of adopting state v. τ_v is the mean life-time and Λ_v the conductance of pore state v. 1407 transitions between neighboring conductance states were analyzed during an observation time of 76.7 sec.

autocorrelation function. As can be seen from Fig. 11*a*, there is a reasonable agreement between the power spectral density and the theoretical curve given by Eq. (17) on the level of single-pore events.

There is evidence that the time constant of the slower process τ_s is correlated to the mean life-time of a single-pore. Statistical analysis of the record of current fluctuations used for the computation of $C(\tau)$ and $S(f)$ shown in Fig. 11*a* (part of the corresponding conductance fluctuations are shown in Fig. 10*a*) yields a mean life-time of single-pores τ_b of about 200 msec. This value was calculated from the analysis of 350 pores. It turned out that the number of short-lived pores with the pattern of a single spike (*see also* Fig. 10*a*) is larger than expected from an exponential distribution of life-times. Their occurrence will be discussed later. The value of τ_b agrees closely with the correlation time $\tau_s=190$ msec obtained for the slower process from autocorrelation analysis.

Furthermore, we analyzed the conductance fluctuations arising from transitions between different neighboring conductance states within *one* pore. Fig. 10*b* shows the conductance pattern of one pore which exhibits conductance transitions between different pore states v over a longer time range. If the nonconducting pore state is denoted by $v=0$ and the following conducting states denoted by $v=1, 2, 3, \ldots$, it can be seen from Fig. 10*b* and Table 4 that the pore states with a higher probability of occurrence p_v are $v=3, 4$ and 5. Fig. 11*b* shows the power spectral density and the autocorrelation function (inset) of *one* pore as shown in Fig. 10*b*. In both cases only a single time-dependent process of a time constant in the ms-range occurs. A similar behavior of the autocorrelation function was

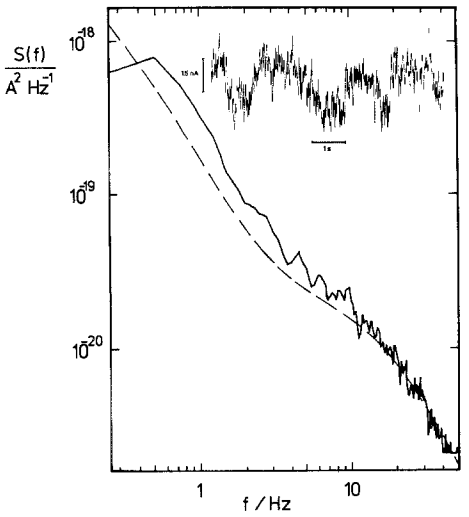

Fig. 12. Power spectral density $S(f)$ of the current noise generated by an alamethicin-doped black lipid membrane versus frequency f. Part of the corresponding current noise is shown in the inset. The power spectrum density shown is an average of 64 spectra. The mean membrane conductance was $\lambda_\infty = 51\ \mu S\ cm^{-2}$, membrane area $7.1 \times 10^{-3}\ cm^2$ and applied voltage 50 mV. The theoretical curve was drawn according to Eq. (17) using the values of C_s, C_f, τ_s and τ_f determined by the simultaneously processed autocorrelation function $C(\tau)$ shown in Fig. 1*a*. For further explanations *see text. Inset:* Current noise generated by 1% dioleoyllecithin in *n*-decane in the presence of alamethicin (250 ng/cm³) at 11 °C, 1 M KCl and an applied voltage $V = 50$ mV

observed for the case of gramicidin A-doped lipid membranes (Kolb *et al.*, 1975).

$C(\tau)$ shown in Fig. 11*b* may be described by Eq. (1) using $C_s = 0$ and the parameter values $C_f = 1.5 \times 10^{-20}\ A^2$ and $\tau_f = 44$ msec. Using these parameters obtained by autocorrelation analysis for calculation of the power spectral density from Eq. (17) (dashed curve in Fig. 11*b*) we find close agreement with the measured power spectral density. The same record which was used for processing $C(\tau)$ and $S(f)$ was plotted by a strip chart recorder. From a statistical analysis of this record the life-times τ_ν of the pore states ν were calculated (Table 4). As can be seen from Table 4 the life-times τ_ν are in the range of 29 to 69 msec. The average and weighted mean value of τ_ν lies within this range and is closely related to the correlation time $\tau_f = 44$ msec.

The inset of Fig. 12 shows the fluctuating component δJ of the membrane current $J(t)$ induced by a multi-pore system of an alamethicin-doped lipid membrane at 11 °C, 1 M KCl and $V = 50$ mV. As may be seen from

the conductance-voltage relation shown in Fig. 2 the applied voltage leads to a conductance which lies within the range of voltage-dependent conductances. The corresponding autocorrelation function is shown in Fig. 1*a* and the power spectral density in Fig. 12. As observed in the presence of single alamethicin pores (Fig. 11*a*) both functions show two processes of different time behavior. A fit of the measured power spectral density by Eq. (17) using the corresponding values of $C(\tau)$ (*see* Fig. 1*a*) shows poor agreement especially at lower frequencies. In all cases an underestimate compared with the measured power spectral density was observed. It was found that this deviation is less pronounced in the case of higher temperatures where both the slow and fast process appear at higher frequencies.

Discussion

In the previous section it was shown that under voltage-clamp conditions the autocorrelation function of alamethicin-induced current fluctuations may be described by a linear superposition of two exponential functions. The main problem of autocorrelation analysis consists in assigning the empirical parameters of the autocorrelation function (the amplitudes and correlation times) obtained from a steady-state multi-pore system to molecular parameters of the single-pore. The assignment will be done phenomenologically by comparison of the results of autocorrelation analysis performed on the single-pore and multi-pore level with those from the statistical analysis of single-pore experiments and from multi-pore relaxation experiments described in part I (Boheim & Kolb, 1977). Comparison of the autocorrelation function defined by Eq. (11) with the observed function given by Eq. (1) leads to the hypothesis that the autocorrelation function should arise from at least two sources of spontaneous microscopic conductance fluctuations. The experiments of Eisenberg *et al.* (1973) who statistically analyzed the alamethicin-induced conductance fluctuations at moderate conductance levels up to about 2 μS give evidence that the observed conductance fluctuations arise from fluctuations in the number of pores as well as from fluctuations in the states of individual pores. For an interpretation of the results presented in the previous section we want to confirm the assumption that the two components of the autocorrelation function result from fluctuations in the number and in the states of the pores, respectively. At first in the case of multi-pore systems we restrict ourselves to the range of voltage-dependent conductance.

The Slow Process

The slow correlation process which occurs in the range of 10 msec to 5 sec exhibits a strong voltage dependence. Eisenberg *et al.* (1973) observed a relaxation process with alamethicin-doped phosphatidyl-ethanolamine/*n*-decane membranes of similar time scale and voltage dependence. In order to compare correlation and relaxation processes we use the fluctuation-dissipation theorem (Kubo, 1957). It states that the decay of a spontaneous fluctuation follows on the average the same time-law as the relaxation from a macroscopic perturbation. A comparison of relaxation and corresponding correlation times on the basis of this theorem is only reasonable if the system under investigation exhibits identical steady-state properties in both types of measurements. This means that in the case of relaxation experiments the steady-state which is adopted after the relaxation process has to be equivalent to the state of the system in which the autocorrelation function is recorded. The relaxation experiments described in part I show that the absolute values of the slow relaxation time as well as the voltage dependence of this process are to some extent dependent on the choice of pretreatment procedure of the membrane system before applying a voltage-jump. In the following we want to compare the voltage-pretreatment conditions of alamethicin-doped lipid membranes at which correlation analysis (this paper) and relaxation experiments (Boheim & Kolb, 1977) were performed. In the case of autocorrelation experiments following a zero voltage-pretreatment for 90 min the voltage-conductance relation $\lambda_\infty(V)$ was recorded by *increasing* the voltage in steps of 5 mV. After an equilibration time of about two minutes the mean membrane conductance was measured during another 50–90 sec as described in the previous section. Concerning the relaxation experiments we want to compare with those experiments where the voltage-jump was applied from zero to the final voltage after the same zero voltage-pretreatment of the membrane which was denoted by low λ_Φ-pretreatment in part I. The successive voltage-jumps were carried out with *decreasing* amplitude; after relaxation of the system to the new steady-state the final conductance λ_∞ was measured. Despite the fact that for both methods the function $\lambda_\infty(V)$ was recorded differently the results are comparable as shown below. If the slope of $\log\lambda_\infty$ *vs.* V is expressed in terms of $\alpha[\lambda_\infty]$ [Eq. (4)] both methods yield the same rate of increase with decreasing temperature (Table 1 of parts I and II, respectively). The absolute values of $\alpha[\lambda_\infty]$ obtained from the autocorrelation functions as compared with those from the relaxation experiments are systematically shifted by about 5% to higher

values. This variation could be explained by the fact that the voltage-pretreatment of the membrane in the case of relaxation experiments is different from that used for autocorrelation analysis. At higher conductances $\lambda_\infty \gtrsim 1$ mS cm^{-2} a saturation behavior of $\lambda_\infty(V)$ was observed under steady-state conditions (Fig. 2). In case of current-relaxation experiments this behavior of $\lambda_\infty(V)$ was obtained after high λ_Φ-pretreatment of the membrane, by applying a distinct voltage within the voltage-dependent conductance range to the membrane, but not for low λ_Φ-pretreatment. Both experimental methods yield a similar dependence of λ_∞ on the alamethicin and salt concentration at constant voltage. According to Eq. (5) we found for the alamethicin concentration dependence at 11 °C and 1 M KCl $\delta[\lambda_\infty]=9.8$ from autocorrelation experiments and $\delta[\lambda_\infty]=11.5$ from relaxation experiments; for the salt concentration dependence from autocorrelation experiments it is found $\varepsilon[\lambda_\infty]=5.8$ at 25 °C and $\varepsilon[\lambda_\infty]=7.9$ at 11 °C compared to $\varepsilon[\lambda_\infty]=4.0$ at 25 °C and $\varepsilon[\lambda_\infty]=7.9$ at 11 °C in case of relaxation experiments. Owing to the satisfying agreement of the steady-state properties of the systems at which the autocorrelation and relaxation measurements were carried out, the fluctuation-dissipation theorem is applicable for a comparison of the corresponding time constants.

The voltage dependence of the slow relaxation time and of the slow correlation time expressed in terms of $\alpha[\tau_s]$ [Eq. (7)] agrees closely. $\alpha[\tau_s]$ shows the same rate of increase with decreasing temperature independent of alamethicin concentration in both cases (Table 1 of parts I and II, respectively). The absolute values of τ_s shift to higher values with increasing alamethicin concentration at constant voltage. If this concentration dependence is described in terms of $\delta[\tau_s]$ [Eq. (9)] we find $\delta[\tau_s]=4.6$ and $\delta[\tau_s]=3.9$ at 11 °C and 1 M KCl for the autocorrelation and relaxation analysis, respectively. For the ratio $\delta[\tau_s]/\varepsilon[\tau_s]$ where $\varepsilon[\tau_s]$ indicates the salt concentration dependence of τ_s [Eq. (10)] we obtained the values 1.6 (autocorrelation analysis) and 2.1 (relaxation experiments, Table 3 of part I), respectively, at 11 °C. The closely related results for the voltage, alamethicin concentration and salt concentration dependences of the slow correlation time and slow relaxation time indicate that both time constants are related to the same kinetic parameters.

A possible explanation for the slow relaxation process has been proposed by Eisenberg *et al.* (1973). They assumed that this process of first order is connected with the formation and the decay of pores. As discussed in part I, the corresponding relaxation time should be identical with the mean life-time of a fluctuating pore. This assignment is confirmed by the results obtained by statistical and autocorrelation analysis of con-

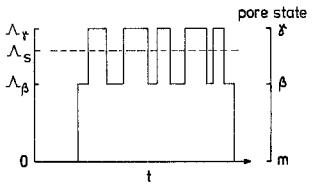

Fig. 13. Simplified model of alamethicin-induced conductance fluctuations versus time t of a single conducting pore. The pore can adopt the states m, β and γ, whereby m refers to the nonconducting pore state. Λ_γ and Λ_β are the conductance levels of the corresponding pore states γ and β, respectively. Λ_s is the mean pore conductance

ductance fluctuations induced by single pores (Fig. 10*a*). As described in the previous section the correlation time τ_s of the slow process (Fig. 11*a*) agrees closely with the mean pore life-time τ_b obtained by statistical analysis from the same record of events. Further evidence for this explanation of the slow process may be obtained from the absolute value and the voltage dependence of the corresponding amplitude of the autocorrelation function. In the case of gramicidin A-doped lipid bilayers it was shown (Kolb *et al.*, 1975) that the amplitude of the autocorrelation function could be related to the mean value of the single-channel conductance. The relationship between both quantities could be calculated on the basis of a simple two-state model of channel formation. In order to obtain a similar relation between the variance of alamethicin-induced conductance fluctuations and single-pore conductances, we describe in the following the multi-state behavior of an alamethicin pore by a simplified two-step mechanism consistent with the experimental finding of two correlation times of different voltage dependence. It is assumed that the voltage-dependent step is related to the pore formation and decay which may be described by the reaction

$$A_m \underset{k_{\beta m}}{\overset{k_{m\beta}}{\rightleftharpoons}} A_\beta. \tag{18}$$

This is schematically presented by the scheme given in Fig. 13, where A_m denotes the inactive pores, A_β the conducting pores of state β, $k_{m,\beta}$ and $k_{\beta,m}$ the rate constants of forward and backward reaction between the states m and β, respectively. The second step in this model is a voltage-independent transition to an adjacent conductance state γ:

$$A_\beta \underset{k_{\gamma,\beta}}{\overset{k_{\beta,\gamma}}{\rightleftharpoons}} A_\gamma, \tag{19}$$

where A_γ denotes the conducting pores in state γ, $k_{\beta,\gamma}$ and $k_{\gamma,\beta}$ the rate constants of forward and backward reaction between the states β and γ,

respectively. The pore states β and γ should comprise those states of the multi-state alamethicin pore which show the highest probability of occurrence. As shown in the Appendix, within the model outlined above, the strong voltage dependence of the slow correlation time τ_s is determined by the rate constants $k_{\beta,m}$, $k_{m,\beta}$ [*see* Eq. (A.9)]. The corresponding conductance fluctuations are related to the pore conductance Λ_s according to Eq. (A.17). On the other hand, the steady-state conductance λ_∞ may be described by the relation:

$$\lambda_\infty(V) \cdot A = L \cdot \bar{n}_p(V) \cdot \bar{\Lambda}(V) \tag{20}$$

where $\bar{n}_p$ is the mean mole number of conducting pores, $\bar{\Lambda}$ the mean single-pore conductance, A the membrane area and L Avogadro's number. Provided that the slow process is related to fluctuations in the number of pores as discussed above, then it may be seen from a comparison of Eqs. (20) and (A.16) that the pore conductance Λ_s determined by autocorrelation analysis is equivalent to $\bar{\Lambda}$. In the following we want to confirm this assumption. In the case of single-pore experiments $\bar{\Lambda}$ may be obtained by statistical analysis. For the fluctuation pattern of single pores partly shown in Fig. 10*a*, we obtained from 350 pores the estimated value $\bar{\Lambda} = 1.9$ nS. According to Eqs. (A.10) and (A.17) the pore conductance Λ_s can be calculated using the value $C_s = 8.2 \times 10^{-21}$ A^2 obtained by autocorrelation analysis (Fig. 11*a*) and $\lambda_s \cdot A = 0.23$ nS. $\lambda_s \cdot A$ is equivalent to $\lambda_\infty \cdot A$ which was determined by statistical analysis from the same record of conductance fluctuations (Fig. 10*a*) used for processing the autocorrelation function. At an applied voltage of 130 mV we obtain $\Lambda_s = 2.1$ nS which is in close agreement with the value of $\bar{\Lambda}$.

In the case of multi-pore systems the experimental values of Λ_s are given in Fig. 8*a*. For the voltage dependence of the mean pore conductance expressed in terms of $\alpha[\Lambda_s]$ in analogy to Eq. (4) we found, independent of temperature, alamethicin and ion concentration in the range of 0.1 to 1 M KCl, a value of $\alpha[\Lambda_s] = 0.4 \pm 0.1$. This value which was obtained from a multi-pore system in di-(18:1)-lecithin membranes is in close agreement with the voltage-dependence of the mean conductance $\bar{\Lambda}$ of a single-pore in a di-(22:1)-lecithin membrane, where $\alpha[\bar{\Lambda}] \approx 0.35$ was obtained (Boheim, 1974). According to the relation

$$\Lambda_s = \bar{\Lambda} = \sum_\nu p_\nu \Lambda_\nu \tag{21}$$

where p_ν is the probability of occurrence of state ν and Λ_ν the corresponding conductance, the experimentally determined dependence of Λ_s on voltage

is consistent with the interpretation that Λ_v remains virtually constant within the considered voltage range, whereas the p_v distributions shift to higher pore states with increasing voltage (Boheim, 1974). Since Λ_s remains virtually constant the plots of the parameters τ_s, τ_f, C_s and C_f determined by autocorrelation analysis versus λ_∞ are according to Eqs. (20) and (21) plots virtually versus N_p, the number of pores. Therefore at constant λ_∞ scatter of these quantities, which possibly arise from variations of C_{AL} at the membrane-water interphase, are partially compensated by variations of the applied voltage, so that N_p remains virtually constant. The less scatter found if these parameters are plotted versus λ_∞ instead of V indicates that τ_s, τ_f, C_s and C_f are mainly dependent on N_p and to a lesser extent on V.

The absolute value of Λ_s determined from autocorrelation analysis at 1 M KCl, 11 °C, 250 ng/cm^3 alamethicin and $V=50$ mV yields $\Lambda_s=1.1 \pm 0.2$ nS. From the single-pore data presented in part I, $\bar{\Lambda}$ may be estimated as follows. Using Eqs. (A.16) and (A.18) of part I and the value of $\delta[\tau_s]=4.2$ we find for the mean pore state $\bar{\nu}\approx 3.7$ whereby the pore state $\nu=0$ (ν can adopt the values 0, 1, 2, 3, ...) corresponds to the nonconducting pore state. The mean single-pore conductance $\bar{\Lambda}$ may be estimated from the results of single-pore experiments according to the relation $\bar{\Lambda}\approx\Lambda_{\bar{\nu}}$, where $\Lambda_{\bar{\nu}}$ denotes the conductance which corresponds to the mean pore state $\bar{\nu}$. Using the values of Λ_ν at $\bar{\nu}=3.7$ (*see* Fig. 1 *a* of part I) we obtain $\bar{\Lambda}\sim 2.6$ nS at $V=100$ mV. The comparison shows that in the case of the multi-pore system $\bar{\Lambda}$ obtained by autocorrelation analysis is about half the value as estimated from single-pore experiments. As pointed out in part I, the value of Λ_ν seems to increase with increasing incubation time. As a tentative explanation this effect could be caused by an increase of the mean length of the α-helix of alamethicin monomers in contact with the hydrophobic membrane interior (Jung, Dubischar & Leibfritz, 1975) which would lead to a shortening of the β-bend part and/or by a thinning of the membrane. In single-pore experiments a few pores of higher conductances Λ_ν are excited by applying a voltage than in the case of multi-pore experiments. This variation might arise from a distribution of monomers with respect to the length of the α-helix, whereby molecules with a larger α-helix are more likely inserted into the membrane.

As Fig. 8 *a* shows Λ_s remains constant within experimental error for a temperature range from 11 to 25 °C. Fig. 8 *a* indicates that according to Eq. (21) Λ_ν and p_ν should change as functions of temperature in such a way that Λ_s remains constant. In part I it was shown that Λ_ν increases with increasing temperature, therefore p_ν has to decrease just leaving Λ_s constant.

The Fast Process

From the statistical analysis of single-pore events there is now considerable evidence that the conducting pore consists of several aggregated alamethicin molecules. After formation of a pore it first adopts its lowest conductance level and thereafter higher states in a consecutive sequence (Eisenberg *et al.*, 1973; Boheim, 1974; Gordon & Haydon, 1975, 1976). The probability distribution p_ν of the pore states ν calculated from single-pore events shows that a pore adopts the 2–3 most probable states during 70–90% of its life-time (Boheim, 1974). Therefore it seems reasonable to assume that transitions between these most probable conductance levels give the main contribution to the autocorrelation function. It is shown in Table 4 from the statistical analysis of a single-pore that the mean life-times τ_ν of the three most probable pore states $\nu=3,4,5$ (at 4°C and 1 M KCl) are quite similar. The absolute values of the fast correlation time τ_f and the mean life-times τ_ν at 11 °C (part I) differ by a factor of about three, but both quantities exhibit an activation energy of about 12 kcal/mol. From the statistical analysis of single-pores (Boheim, 1974) only a weak voltage dependence of the mean life-time τ_ν of the most probable pore state ν is obtained and a similar behavior is found for τ_f (Fig. 4*b*). Further support for the assignment that the fast decaying component of the autocorrelation function arises from transitions between the most probable conductance states of a single-pore described by Eq. (19) comes from the analysis of the autocorrelation amplitudes obtained from the following experiments. First we carried out the autocorrelation analysis of current fluctuations of a single pore which were only generated by transitions between different states of conductance (Fig. 10*b*). In this case the autocorrelation function exhibits a single exponential behavior (Fig. 11*b*). The corresponding correlation amplitude C_f can be related to the mean value of the conductance difference $\overline{\Lambda_{\nu+1}-\Lambda_\nu}$ between neighboring conductance levels $\Lambda_{\nu+1}$ and Λ_ν according to the relation [Kolb *et al.*, 1975; *see also* Eq. (A.17)]:

$$\frac{C_f}{V^2\cdot\lambda_\infty\cdot A}\approx\overline{\Lambda_{\nu+1}-\Lambda_\nu}. \tag{22}$$

In the following we define:

$$\overline{\Lambda_{\nu+1}-\Lambda_\nu}=\overline{\Delta\Lambda_\nu}. \tag{23}$$

As may be seen from Fig. 10*b* in the case of a fluctuating pore the relation $\lambda_\infty\cdot A\approx\overline{\Delta\Lambda_4}=1.1$ nS holds. Using the value $C_f=1.5\times10^{-20}$ A^2

determined at 120 mV (Fig. 11*b*) we obtain from Eq. (22) $\overline{\Delta\Lambda_v} = 0.95$ nS compared to $0.5\,(\Lambda_5 - \Lambda_3) = 1.1$ nS.

In view of this analysis we see that the baseline of the fast fluctuation process is approximately given by the pore state $v = 3$. From this level transitions between the different pore states start. On the other hand, the highest conductance level occurring with high probability is given by $v = 5$, whereas level $v = 4$ indicates the mean value of the conductance fluctuations between the pore states. With regard to the two-step model (Fig. 13) we have to correlate the levels β and γ in the following way to obtain the above given approximated results: $\beta = 3$; $\gamma = 5$.

With

$$\lambda_\infty \cdot A = \frac{(\Lambda_5 - \Lambda_4) + (\Lambda_4 - \Lambda_3)}{2} \approx \overline{\Delta\Lambda_4} \tag{24}$$

and the definition of $(\Lambda_\gamma - \Lambda_\beta)$ (*see* Fig. 13) it follows

$$\overline{\Delta\Lambda}_{\left(\frac{\beta+\gamma}{2}\right)} = \tfrac{1}{2}(\Lambda_\gamma - \Lambda_\beta). \tag{25}$$

In the following we define

$$\Lambda_f = \tfrac{1}{2}(\Lambda_\gamma - \Lambda_\beta). \tag{26}$$

If we choose β and γ in the above given way, the mean difference of neighboring pore states is obtained in a satisfying approximation from the autocorrelation amplitude as demonstrated above for $\overline{\Delta\Lambda_4}$. A comparison of the conductance pattern of a single-pore (Fig. 10*b*) with the simplified model presented in Fig. 13 shows that the mean pore conductance which lies between the pore states $v = 3$ and $v = 5$ at 4 °C (a mean pore state $\bar{v} = 3.8$ is calculated from the data given in Table 4) has to be located between the states β and γ.

As shown in the Appendix in the general case of two coupled processes Λ_f can be calculated from the product of C_f and C_s according to Eq. (26) and Eqs. (A.10) and (A.20). In Fig. 14 Λ_f is plotted as a function of voltage for the multi-pore systems investigated at different temperatures under the assumption of $K = 1$ for equal occupancy of states β and γ. (The estimate $K = 1$ is justified because, according to the definition of states β and γ, the maximum value of p_v is assumed between states β and γ.) Within experimental error Λ_f is virtually voltage-independent. A similar result may be seen for Λ_v obtained from the statistical analysis of single-pore events for the considered voltage interval (Eisenberg *et al.*, 1973; Boheim, 1974). This finding supports the hypothesis based on the model outlined above that

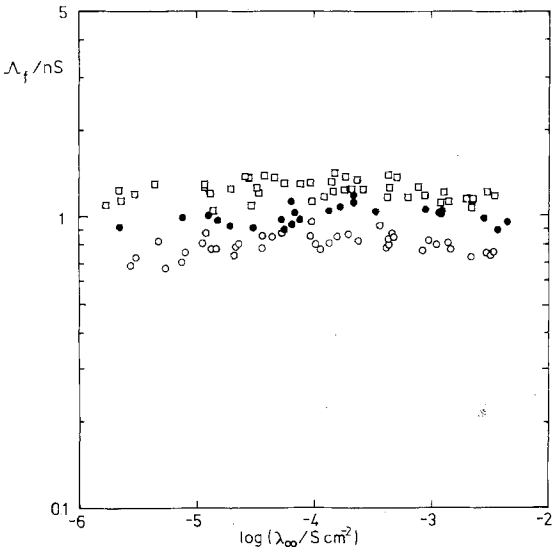

Fig. 14. Λ_f as a function of mean membrane conductance λ_∞ at different temperatures: o, 11 °C; ●, 18 °C; □, 25 °C. Λ_f was calculated from Eqs. (A.20) and (26) using the values presented in Fig. 8*b* and the corresponding data of Fig. 8*a* with $K=1$. For further explanations *see text*. The aqueous phase contained 250 ng/cm^3 alamethicin and 1 M KCl

Λ_f is an estimate for the mean difference of neighboring conductance levels of single pores. Further evidence for this assignment may be seen from a comparison of the corresponding activation energies; we find $E(\Lambda_f)\approx 5$ kcal/mol and $E(\Lambda_v)\approx 4$ kcal/mol (part I). In order to compare the values of Λ_s and Λ_f with corresponding values obtained from single-pore experiments and because the absolute values differ by a factor $\gtrsim 2$ we use the ratio Λ_s/Λ_f which is given from Eqs. (A.10), (A.17) and (A.20) by

$$\frac{\Lambda_s}{\Lambda_f}=\frac{2}{1+K}\cdot\sqrt{\frac{K\cdot C_s}{C_f}}. \tag{27}$$

Using $K=1$ (*see above*) we find at 11 °C and an applied voltage of 60 mV the value $\Lambda_s/\Lambda_f\approx 1.4$. From the statistical analysis of single alamethicin pores in di-(22:1)-lecithin membrane at 11 °C and $V=63$ mV, $\bar{\nu}=3$ (Boheim, 1974) we can calculate the corresponding ratio $\bar{\Lambda}/\overline{\Delta\Lambda_\nu}$ yielding the value 1.5. The analysis in di-(18:1)-lecithin membranes (part I) shows that the data are also in agreement with $\bar{\nu}=3$. This value is similar to $\bar{\nu}=3.7$ estimated above. At 25 °C we obtain from multi-pore experiments the ratio $\Lambda_s/\Lambda_f\approx 1.0$. This implies that the conductance level $\bar{\nu}=2.3$ of the pore is preferentially adopted. From Eqs. (A.16), (A.17) and (18) of part I and the data of Table 1 (this paper) we obtain $\bar{\nu}\approx 2.6$.

Recently Moore and Neher (1976) have published an autocorrelation function of an alamethicin-modified dioleoyl-L-α-lecithin/cholesterol/*n*-decane membrane at $V = 50$ mV, 1 M KCl, 10^{-8} M alamethicin and 21–23 °C. They reported about a single correlation process of a time constant of about 8 msec (estimated from Fig. 6 of their publication). This correlation time lies in the range of the time constant we found for the fast process. Under comparable experimental conditions of Moore and Neher we found for dioleoyl-L-α-lecithin/*n*-decane membranes $\tau_f \approx 4$ msec. As might be seen from Fig. 4*b* one should expect a second slower correlation process with a time constant of about 0.1 sec.

As pointed out above the correlation amplitude of the slow process should be related to the mean conductance of a single alamethicin pore. But as Eq. (A.20) shows the correlation amplitude of the fast process which is generated by fluctuations between different conducting states of a given pore cannot directly be related to a mean unit step conductance. Therefore, the assignment described by Moore and Neher (1976) of the ratio of the fast correlation amplitude C_f^* and the mean steady-state conductance $\lambda_\infty \cdot A$ to a weighted average of the multiple conductance levels is incorrect as in the case of alamethicin two coupled processes exist.

Range of Weakly Voltage-Dependent Conductance

In the range of weakly voltage-dependent conductance we observe a strong increase of τ_s, τ_f (Fig. 4*a*) and Λ_s (Fig. 7). As may be seen from the values of C_f^* and C_s^* for this conductance range (Fig. 7) using Eqs. (A.20) and (26) also Λ_f strongly increases. The absolute values of τ_f and τ_s are up to a factor of 5–7 lower than the corresponding correlation times measured at the beginning of the voltage-dependent conductance range. The slow and fast processes observed in the range of weakly voltage-dependent conductance seem to represent a different kind of alamethicin-induced conductance fluctuations as described above for the voltage-dependent range of conductance. If we use the relation given by Eq. (20) for λ_∞ and the values of Λ_s obtained for the range of weakly voltage-dependent conductance (Fig. 7), we find a decreasing number of pores with increasing conductance in this range. A tentative explanation of this finding may be given on the basis of the mechanism of preaggregate and pore nucleus formation proposed in part I. The alamethicin concentration dependence of the pore formation rate μ expressed in terms of $\delta[\mu]$ was found to be about 6 for the range of voltage-dependent conductance

(Table 2 of part I). As was pointed out this exponential factor has to be less than or equal to $\delta[\lambda_\infty]$ and reflects the mean number of molecules incorporated in a preaggregate. Roy (1975) reported for the range of weakly voltage-dependent conductance the value $\delta[\lambda_\infty] \approx 2$ to 3. If the proposed relationship between $\delta[\mu]$ and the number of constituents of the preaggregate is applied also for this conductance range the relation $\delta[\lambda_\infty] \gtrsim \delta[\mu]$ would imply preaggregates consisting on the average at the most out of 2 to 3 alamethicin molecules. A tentative explanation of the findings mentioned above will therefore be given on the basis of preaggregates of variable size. With increasing voltage the number of pores preferentially generated from preaggregates of larger size could cause a decrease of the number of preaggregates with a lower number of constituents leading to a decrease of the mean number of conducting pores. The strong increase of the correlation times as well as the correlation amplitudes with increasing conductance in the range of weakly voltage-dependent conductance which is significantly different from that found in the range of voltage-dependent conductance could be explained by a faster kinetic behavior of short-living pores formed from small preaggregates. Further evidence for this interpretation may be given by the single-pore experiments described above. The fast correlation time obtained from a single-pore fluctuating for a long time between neighboring pore states yielded 46 msec (Fig. 11 *b*) whereas the fast correlation time obtained from different relatively short-living single-pores yielded 21 msec (Fig. 11 *a*). In the latter case the faster correlation time may be caused by the appearance of short-living spikes always observed on the single-pore level (Fig. 10 *a*) of only one or two conducting states of lower amplitude as compared to the pores which exhibit a clear distinguishable pattern of different conducting levels.

Range of High Conductances

In the range of high conductances $\lambda_\infty \gtrsim 1$ mS cm^{-2}, we observe a saturation behavior of λ_∞ (Fig. 2) as well as of the slow correlation time τ_s whereas τ_f remains unchanged (Figs. 4 *a* and *b*) in accordance with the results obtained from the corresponding relaxation experiments (part I). Using the data presented in Figs. 2 and 4 *a* it may be seen that the formation rate μ remains nearly constant in this conductance range. Furthermore the finding of a constant mean single-pore conductance (Fig. 7) implies a restriction in the size of the alamethicin pores with increasing voltage. A constant pore size would be consistent with the observation of a constant

mean life-time τ_s of the pores. A likely explanation of the saturation behavior may be given if the pores of the multi-pore system interact, i.e. no longer fluctuate statistically independent. Using the relation (A.16) and the data of Fig. 7 we obtain a mean distance of the pores of about 500 Å which seems too large for an interaction of the pores. But an interaction of the pores could occur if they are present in clusters as proposed for multi-pore systems of gramicidin A-modified lipid membranes (Kolb & Bamberg, 1977). Another possible explanation would be given by a limited number of active monomers in this conductance range (part I).

Ion Concentration Dependence

In the following we consider the dependence of the autocorrelation function on ion concentration measured in the range of 1 to 0.1 M KCl. We restrict ourselves to the range of voltage-dependent conductance and consider the dependence of τ_s and τ_f on ion concentration at constant membrane conductance but varying number of pores N_p. A decrease of the ion concentration by one order of magnitude causes an about eightfold decrease of the mean pore conductance Λ_s [*see* Eq. (A.17) and Fig. 9]. At constant membrane conductance this implies according to Eqs. (20) and (21) an about eightfold increase of the mean pore number $\bar{N}_p$. This situation is similar to that at constant ion concentration where a 10-fold increase of λ_∞ causes an equivalent increase of $\bar{N}_p$ since Λ_s remains virtually constant (Fig. 8*a*). However, as might be seen from Fig. 4*b* an increase of $\bar{N}_p$ by one order of magnitude causes an increase of τ_s by about a factor of three slightly dependent on temperature whereas τ_f remains almost constant. Therefore, a similar increase of τ_s would have to be expected for an increase of $\bar{N}_p$ in the ion concentration range of 1 M to 0.1 M. As Fig. 6*b* shows τ_s increases for an ion concentration change from 1 to 0.5 M but at lower concentrations τ_s as well as τ_f decreases. A tentative explanation for this finding may be given by an electrostatic influence of the ionic strength on the kinetic parameters of a single-pore as observed in the case of gramicidin A-doped lipid membranes (Kolb & Bamberg, 1977). In the latter case an electrostatic stabilization of the channel leading to longer pore life-times with an increasing ionic strength was proposed.

The mean pore conductance was found to vary linearly on a log/log scale with a slope of 0.8 within this ion concentration range (Fig. 9). A similar result may be obtained for $\overline{\Delta\Lambda_v}$ using the experimental values shown in Fig. 9 and the Eqs. (A.20) and (25). This implies that the prob-

abilities p_ν of the pore states ν remain virtually constant within this ion concentration range whereas Λ_ν varies with a constant slope of 0.8 which is in agreement with the results of Eisenberg *et al.* (1973).

The authors wish to thank Prof. P. Läuger for helpful discussions and for critically reading the manuscript. This work has been supported by the Deutsche Forschungsgemeinschaft (Sonderforschungsbereich 138).

Appendix

In the following we give a derivation of the correlation times τ_s and τ_f and of the pore conductances Λ_s and $\Lambda_\gamma - \Lambda_\beta$ based on the model schematically presented in Fig. 13 and described by the two reaction steps of Eqs. (18) and (19).

Correlation Times

According to the fluctuation-dissipation theorem (Kubo, 1957) the correlation times may be calculated from the corresponding relaxation processes. If the second reaction [Eq. (19)] is much faster than the first one, the differential equation for the fast step is given by:

$$\frac{dc_\gamma}{dt} = k_{\beta,\gamma}\, c_\beta - k_{\gamma,\beta}\, c_\gamma \tag{A.1}$$

where c_β and c_γ are the concentrations of the conducting pores in state β and γ, respectively. As the total concentration of pores does not change during the fast process it is obvious that

$$\Delta c_\gamma = -\Delta c_\beta \tag{A.2}$$

for the change of the equilibrium concentration of $\bar{c}_\beta$ and $\bar{c}_\gamma$, respectively. Substituting $\bar{c}_\beta + \Delta c_\beta$ for c_β and $\bar{c}_\gamma + \Delta c_\gamma$ for c_γ in Eq. (A.1) and employing Eq. (A.2) leads to the fast correlation time

$$\tau_f^{-1} = k_{\beta,\gamma} + k_{\gamma,\beta}. \tag{A.3}$$

The initial slow reaction step [Eq. (18)] requires besides Eq. (A.1) the differential equation:

$$\frac{dc_\beta}{dt} = k_{m,\beta}\, c_m + k_{\gamma,\beta}\, c_\gamma - (k_{\beta,m} + k_{\beta,\gamma})\, c_\beta \tag{A.4}$$

where c_m is the concentration of inactive pores.

Eqs. (A.1) and (A.4) combine to:

$$\frac{dc_p}{dt} = k_{m,\beta}\, c_m - k_{\beta,m}\, c_\beta \tag{A.5}$$

where c_p denotes the concentration of conducting pores given by the relation:

$$c_p = c_\beta + c_\gamma . \tag{A.6}$$

Assuming equilibrium between c_β and c_γ according to the relation

$$c_\gamma = K \cdot c_\beta \tag{A.7}$$

where K is the equilibrium constant, one derives from stoichiometry and conservation of mass for the slow process:

$$\Delta c_\gamma = K \cdot \Delta c_\beta . \tag{A.8}$$

If one assumes that during a concentration fluctuation of c_p and c_β the sum of concentrations of inactive pores c_m and active pores c_p is not affected and employs Eqs. (A.6), (A.7) and (A.8) one finds for the slow correlation time τ_s related to fluctuations in the concentration of conducting pores:

$$\tau_s^{-1} = \frac{k_{m,\beta}(1+K) + k_{\beta,m}}{1+K} . \tag{A.9}$$

Pore Conductances

In the Results section it has been shown that owing to the different time scales of the fast and the slow process the corresponding current fluctuations can be measured separately by selecting appropriate filters. In both cases a single exponential term was obtained for the autocorrelation function. The amplitude of the autocorrelation function is the corresponding variance of the current fluctuations. According to Eqs. (1) and (13) we may write for the amplitude of the autocorrelation function $C(\tau)$:

$$C(0) = C_s + C_f = V^2(\sigma_{\lambda_s}^2 + \sigma_{\lambda_f}^2) \tag{A.10}$$

where $\sigma_{\lambda_s}{}^2$ and $\sigma_{\lambda_f}{}^2$ are the variances of the slow and the fast fluctuating part of the conductance λ, respectively. The variances of conductance will be calculated using the relation (Tolman, 1962):

$$\sigma_n^2 = \frac{kT}{\left(\frac{d^2 G}{dn^2}\right)_{n=\bar{n}}} , \tag{A.11}$$

where n is the mole number of the randomly fluctuating variable and G the Gibb's free energy of the corresponding enclosed system. k is the Boltzman constant and T the absolute temperature. Here the random variables are given by n_m, n_β and n_γ, respectively. For the reaction scheme given by Eqs. (18) and (19) we find:

$$dG = \mu_m\, dn_m + \mu_\beta\, dn_\beta + \mu_\gamma\, dn_\gamma, \tag{A.12}$$

where μ_m, μ_β and μ_γ are the chemical potentials of A_m, A_β and A_γ. Assuming $dn_m \approx 0$ (*see above*) and equilibrium between n_β and n_γ given by the relation:

$$\mu_\beta = \mu_\gamma \tag{A.13}$$

and using Eq. (A.6) we find for the slow process:

$$dG = \mu_\beta \cdot dn_p, \tag{A.14}$$

where n_p is the mole number of conducting pores. Using Eqs. (A.7) and (A.11) we find:

$$\frac{\sigma^2_{n_p}}{\bar{n}_p} = \frac{1}{L}, \tag{A.15}$$

where L is Avogadro's number. As Rice (1944) showed, Eq. (A.15) should be valid for statistical independent pores. If we write for the macroscopic conductance arising from the slow process [*see* Fig. 13 and Eq. (18)]:

$$\lambda_s(t) \cdot A = L \cdot n_p(t) \cdot \Lambda_s \tag{A.16}$$

we find from Eq. (A.15)

$$\Lambda_s = \frac{\sigma^2_{\lambda_s}}{\bar{\lambda}_s \cdot A} \tag{A.17}$$

for the pore conductance related to the slow process. Correspondingly we find for the fast process using Eqs. (A.7), (A.11) and (A.12):

$$\frac{\sigma^2_{n_\gamma}}{\bar{n}_\gamma} = \frac{1}{L \cdot (1+K)}. \tag{A.18}$$

Using for the conductance arising from the fast intrapore transitions between the conductance states β and γ the relation (*see* Fig. 13):

$$\lambda_f(t) \cdot A = L \cdot n_\gamma(t) \cdot (\Lambda_\gamma - \Lambda_\beta) \tag{A.19}$$

we find from Eqs. (A.6), (A.7), (A.16), (A.17) and (A.18) the relation

$$\Lambda_\gamma - \Lambda_\beta = \frac{(1+K)}{\bar{\lambda}_s \cdot A} \cdot \sqrt{\frac{\sigma^2_{\lambda_s} \cdot \sigma^2_{\lambda_f}}{K}} \tag{A.20}$$

for the conductance difference $(\Lambda_\gamma - \Lambda_\beta)$ related to the fast process.

References

Anderson, C.R., Stevens, C.F. 1973. Voltage clamp analysis of acetylcholine produced end-plate current fluctuations at frog neuromuscular junction. *J. Physiol. (London)* **235**:655

Boheim, G. 1974. Statistical analysis of alamethicin channels in black lipid membranes. *J. Membrane Biol.* **19**:277

Boheim, G., Kolb, H.-A. 1978. Analysis of the multi-pore system of alamethicin in a lipid membrane. I. Voltage-jump current relaxation measurements. *J. Membrane Biol.* **38**:99

Conti, F., De Felice, L. J., Wanke, E. 1975. Potassium and sodium ion current noise in the membrane of the squid giant axon. *J. Physiol. (London)* **248**:45

De Felice, L. J., Sokol, B. A. 1976. Correlation analysis of membrane noise. *J. Membrane Biol.* **26**:405

Eisenberg, M., Hall, J. E., Mead, C. A. 1973. The nature of the voltage-dependent conductance induced by alamethicin in black lipid membranes. *J. Membrane Biol.* **14**:143

Fishman, H. M., Poussart, D. J. M., Moore, L. E. 1975. Noise measurements in squid axon membrane. *J. Membrane Biol.* **24**:281

Gordon, L. G. M., Haydon, D. A. 1972. The unit conductance channel of alamethicin. *Biochim. Biophys. Acta* **255**:1014

Gordon, L. G. M., Haydon, D. A. 1975. Potential-dependent conductances in lipid membranes containing alamethicin. *Phil. Trans. R. Soc. London B* **270**:433

Gordon, L. G. M., Haydon, D. A. 1976. Kinetics and stability of alamethicin conducting channels in lipid bilayers. *Biochim. Biophys. Acta* **436**:541

Jung, G., Dubischar, N., Leibfritz, D. 1975. Conformational changes of alamethicin induced by solvent and temperature: A ^{13}C-NMR and circular-dichroism study. *Europ. J. Biochem.* **54**:395

Katz, B., Miledi, R. 1972. The statistical nature of the acetylcholine potential and its molecular components. *J. Physiol. (London)* **244**:665

Khintchine, A. 1934. Korrelationstheorie der stationären stochastischen Prozesse. *Math. Ann.* **109**:604

Kolb, H.-A., Bamberg, E. 1977. Influence of membrane thickness and ion concentration on the properties of the gramicidin A channel: Autocorrelation, spectral power density, relaxation and single-channel studies. *Biochim. Biophys. Acta* **464**:127

Kolb, H.-A., Läuger, P., Bamberg, E. 1975. Correlation analysis of electrical noise in lipid bilayer membranes: Kinetics of gramicidin A channels. *J. Membrane Biol.* **20**:133

Kolb, H.-A., Läuger, P., Bamberg, E. 1976. Comments on: Correlation analysis of membrane noise. *J. Membrane Biol.* **26**:407

Kubo, R. 1957. Statistical-mechanical theory of irreversible processes. I. General theory and simple applications to magnetic and conduction problems. *J. Phys. Soc. Jpn.* **12**:570

Läuger, P., Lesslauer, W., Marti, E., Richter, J. 1967. Electrical properties of bimolecular phospholipid membranes. *Biochim. Biophys. Acta* **135**:20

Mauro, A., Nanavati, R. P., Heyer, E. 1972. Time-variant conductance of bilayer membranes treated with monazomycin and alamethicin. *Proc. Nat. Acad. Sci. USA* **69**:181

Moore, L. E., Neher, E. 1976. Fluctuation and relaxation analysis of monazomycin-induced conductance in black lipid membranes. *J. Membrane Biol.* **27**:347

Mueller, P. 1976. Membrane excitation through voltage induced aggregation of channel precursors. *Ann. N. Y. Acad. Sci.* **264**:247

Mueller, P., Rudin, D. O. 1968. Action potentials induced in bimolecular lipid membranes. *Nature (London)* **217**:713

Poussart, D. J. M. 1971. Membrane current noise in lobster axon under voltage clamp. *Biophys. J.* **11**:211

Pregla, R., Schlosser, W. 1972. Passive Netzwerke. B.G. Teubner, Stuttgart, p. 117

Ralston, A., Wilf, H. S. 1967. Mathematical Methods for Digital Computers. Vol. 2. John Wiley & Sons, Inc., New York, p. 133

Rice, S. O. 1944. Mathematical analysis of random noise. *Bell Syst. Tech. J.* **23**:282

Roy, G. 1975. Properties of the conductance induced in lecithin bilayer membranes by alamethicin. *J. Membrane Biol.* **24**:71

Stark, G., Benz, R., Pohl, G. W., Janko, K. 1972. Valinomycin as a probe for the study of structural changes of black lipid membranes. *Biochim. Biophys. Acta* **266**:603

Tolman, R. C. 1962. The Principles of Statistical Mechanics. Oxford University Press, London, p. 640

Wanke, E., Prestipino, G. 1976. Monazomycin channel noise. *Biochim. Biophys. Acta* **436**:721

Wiener, N. 1930. Generalized harmonic analysis. *Acta Math.* **55**:117

Zingsheim, H. P., Neher, E. 1974. The equivalence of fluctuation analysis and chemical relaxation measurements: A kinetic study of ion pore formation in thin lipid membranes. *Biophys. Chem.* **2**:197